J Elast (2010) 99: 39–73
DOI 10.1007/s10659-009-9229-x

Equilibrium States of Mechanically Loaded Saturated and Unsaturated Polymer Gels

Hua Deng · Thomas J. Pence

Received: 9 July 2009 / Published online: 3 December 2009

Abstract By a gel we mean a system of crosslinked polymer chains mixed together with a low molecular weight liquid. The polymer and liquid components mix in definite proportions as determined primarily by entropic and enthalpic effects. Swollen gels in equilibrium with a surrounding fluid bath in the absence of mechanical load are often described by a generalized Flory-Huggins equation. In this paper we consider the connection between such a treatment and the broader hyperelastic theory that treats the effect of mechanical loading in deforming the gel. A change in the mechanical loading will generally alter the proportion of liquid in the mixture, leading to either fluid loss (swelling reduction) or fluid gain (swelling increase). In such a case the gel reestablishes equilibrium only when the relative motion of the liquid through the polymer has ceased and processes have come to rest. Such processes are inherently dissipative. Our objective is to study how such reestablished equilibria depend upon mechanical load. For quasi-static loadings that give fluid gain, we then consider a situation in which the amount of available fluid is limited. In this case, increasing quasi-static loading may reach a point at which no additional fluid is available for uptake into the gel system. The associated equilibrium then transitions from a state of liquid saturation to a state in which the gel is no longer saturated. We first consider this quasi-static transition in the context of homogeneous deformation where an appropriate hyperelastic analysis shows that the equilibrium mechanical response is inherently stiffer after loss of saturation. We then consider such a transition in the context of inhomogeneous deformation by studying the boundary value problem of an everted tube subject to an axial load. Loss of saturation again leads to an inherently stiffer quasi-static response.

Keywords Hydrogels · Free swelling · Flory-Huggins · Hyperelasticity · Eversion · Liquid saturated gels

Mathematics Subject Classification (2000) 74A20 · 74B20 · 74F10

H. Deng · T.J. Pence (✉)
Mechanical Engineering, Michigan State University, East Lansing, MI 48824-1226, USA
e-mail: pence@egr.msu.edu

H. Deng
e-mail: denghua@egr.msu.edu

1 Introduction

Gels are high molecular weight crosslinked polymer networks immersed in a low molecular weight liquid. When water is the liquid, then these are typically referred to as hydrogels. The liquid can also be organic in nature as for example discussed in Chapter 7 of Treloar's well known treatise *The Physics of Rubber Elasticity* [20]. Although hydrogels would generally be much softer than a rubbery material infused with an organic liquid, both are regarded as gels for the purpose of this paper, and we shall use the term gel throughout in this broad sense.

When the polymer component of the gel is placed in a liquid bath, the amount of liquid taken up into the gel is in a definite proportion to the amount of polymer. This proportion can change on the basis of temperature, chemistry of the fluid bath, mechanical loading, electrical field, and light exposure. An increase or decrease in liquid proportion gives swelling and shrinking, respectively. In such a case the gel reestablishes equilibrium only when the relative motion of the liquid through the polymer has ceased and processes have come to rest. Such processes are inherently dissipative.

Free swelling is swelling that takes place in the absence of mechanical load, including reactive loads supplied by physical constraint. For isotropic gels, such free swelling is purely volumetric. The equilibrium volume of freely swollen polymers that are not crosslinked is often described in terms of the Flory-Huggins equation [5, 6, 12]. The effect of crosslinking introduces additional terms into this equation. This extended Flory-Huggins equation then contains a number of constitutive parameters. By allowing these parameters to depend upon temperature, fluid chemistry, electrical field and light exposure, this framework can be used to describe free swelling equilibrium deformation in a variety of circumstances.

Mechanical loads that promote volume increase generally cause fluid uptake while loads that promote volume decrease generally cause fluid egress. A suitable generalization of the Flory-Huggins framework as given by Flory and Rehner [7] can treat the effect of boundary displacements and external loads upon equilibrium. For example, Treloar [20] describes experiments on swelling of strained rubber in terms of such a generalized framework. This framework also extends to inhomogeneous deformation in which case the stress equations of equilibrium must be satisfied. In this context, Treloar shows how such a Flory-Rehner framework predicts that quasi-static torsional loading of a cylinder leads to fluid loss and hence swelling reduction [19]. Mechanical constraint can also lead to inhomogeneous swelling deformation as studied by Treloar in [21]. In a similar fashion, Rajagopal, Wineman and collaborators analyze the quasi-static fluid redistribution in a porous elastomer where the redistribution occurs on the basis of either inhomogeneous quasi-static torsional deformation [9] or inhomogeneous quasi-static twisting deformation [23].

The treatments [9, 19, 21, 23] describe equilibrium situations in which both the fluid component and the polymer matrix component of the system are at rest. In particular, each material point in the gel is regarded as a two component mixture of polymer matrix and interpenetrating liquid. Once equilibrium has been attained there is no relative motion between the fluid and matrix components so it is not necessary to invoke the broader continuum mechanical framework that specifically deals with separate mechanical balance principles for each component. This broader framework is known by a number of names, including: the theory of interacting continua, and large deformation mixture theory [15]. Of course, such broader frameworks can also be used to analyze equilibrium in which case the lack of relative motion between the fluid and matrix simplifies the resulting treatment (viz. [9, 23]). Alternatively, the equilibrium can be analyzed directly without invoking the full mixture theory framework [19, 21], which has the additional advantage of making for a

more straight forward specification of boundary conditions. On the other hand, a framework such as mixture theory is required during the time that dissipative processes are operative prior to equilibrium. Examples of mixture theory type treatments for describing the dynamical process of time dependent swelling include [1, 8, 16] where a major focus is on how the liquid component diffuses within the elastomeric matrix.

Our exclusive focus in this paper is on equilibrium states. Thus any reference to loading in this paper is to be understood in a quasi-static sense. To describe real loadings in this way thus requires that the system is close to equilibrium at all times. We further assume that there is negligible hysteresis in the equilibrium mechanical response.[1] This permits a hyperelastic treatment in which there is an underlying notion of energy minimization. Such an assumption by itself amounts to placing certain requirements on the nature of the dissipative processes that govern the approach to any reestablished equilibrium [14].

Here we consider equilibrium states associated with quasi-static mechanical loadings that can lead to both fluid loss (swelling reduction) and fluid gain (swelling increase). For loadings that give fluid gain, a gradually increasing load draws an ever increasing amount of fluid into the gel. If the total amount of available fluid is limited, then it will eventually be the case that no additional fluid is available for uptake into the gel system. From this point on, the overall fluid content of the gel system remains fixed at a value below that associated with liquid saturation. We shall refer to such gels as being nonsaturated.[2] Thus in such a case the system transitions from a state of saturation to a state of nonsaturation at a particular point on the quasi-static load path. It is the object of this paper to discuss various aspects of the hyperelastic modeling of such an equilibrium transition.

In extending the original Flory-Huggins framework so as to incorporate the effect of polymer network elasticity and mechanical loading, one must supply a constitutive model for the hyperelastic properties of the polymer matrix component of the gel system. Motivated by the previous works [9, 19, 21, 23], we develop examples where this aspect of the constitutive model is supplied by the well known Mooney-Rivlin form. Both the polymer matrix component and the fluid component of the gel system are regarded as individually incompressible when isolated from the other component. However the equilibrium response of the overall gel system, so long as it is saturated, can then be described in terms of a hyperelastic framework in which the gel system is nominally compressible. This is because a fixed amount of polymer component can be regarded as defining a gel "element". The amount of fluid component within such a gel element is not fixed, so that fluid flowing in or out of the gel element causes a change in its volume. In other words, compressibility arises as a consequence of the open nature of the gel element. This is in keeping with Treloar's treatment. He writes in [20] that if a rubber that is incompressible in the absence of a liquid swelling agent is subsequently swollen, then the

> ... swollen rubber in continuous equilibrium with a surrounding liquid may be regarded, from the purely formal standpoint, as having mechanical properties equivalent to those of a compressible material.[3]

In particular, since the rubber that is referred to in the above quote is regarded as being in contact with a liquid bath, the situation refers to a state of liquid saturation. Thus the

[1] There would certainly be hysteresis in the time dependent non-equilibrium response.

[2] Alternatively, we could could say that such gels are unsaturated, however we refer to such gels as nonsaturated in this paper (with the exception of the title).

[3] A longer extract from [20] containing this prescient quote is given in [15].

saturated equilibrium response is formally described by a single stored energy density function. This stored energy function has a Flory-Huggins contribution (which only depends on volume change) and a contribution that reflects the elastic properties of the polymer matrix (which, as mentioned above, we take to be of Mooney-Rivlin form). The saturated Cauchy stress tensor then follows from this stored energy density as in compressible hyperelasticity. The local volume change in the deformation then directly correlates to the local change in fluid content.

We first consider load induced transition between liquid saturation and lack of liquid saturation in the context of homogeneous deformation. The relevant stress vs. stretch quasi-static response with liquid saturation is examined for the separate cases of uniaxial loading, equibiaxial loading and equitriaxial loading. For some of these standard loadings, certain choices of the constitutive parameters give rise to nonmonotone relations among: the various stress components, the stretches, and the volume change. This may point to the need to consider alternative constitutive forms in the modeling of any specific gel system. For our purposes, however, this wide range of phenomena exposes a variety of qualitative mechanical responses which may be of interest.

These quasi-static loadings generate changes in the gel volume due to a changing fluid content, and we consider the transition to a nonsaturated response in the event that the gel volume reaches a threshold value determined on the basis of the amount of available fluid. No further overall volume increase may take place once the threshold has been attained. This volume constraint gives rise to an overall confining pressure. Continued quasi-static loading may allow the now fixed amount of fluid in the gel to redistribute spatially, so long as the overall volume is conserved. For the fluid distribution to vary spatially, it is necessary for the stresses to vary spatially.

For homogeneous deformation the amount of fluid is the same everywhere. For homogeneous deformation after such a loss of saturation, the spatially constant local fluid content is completely determined on the basis of the amount of originally available fluid. Thus, echoing Treloar, the nonsaturated quasi-static mechanical properties of the gel under homogeneous deformation are, from the purely formal standpoint, equivalent to those of an incompressible material where the fixed local volume is the specific threshold volume.[4] Stress vs. stretch quasi-static response curves for nonsaturation can be calculated for any desired value of the threshold volume. Any such nonsaturated response curve can be regarded as branching off of the original saturated response curve. Hence the saturated response curve serves as a "backbone" curve such that the various nonsaturated response curves then branch off of this backbone curve. The nonsaturated response is inherently stiffer than the saturated response. In particular, the nonsaturated stress–stretch response curves have greater slope than the saturated response curves at the branching points.

Similar considerations govern inhomogeneous deformation, in which case it is necessary to construct solutions to relevant boundary value problems. For saturated response, the treatment remains formally identical to the conventional hyperelastic theory as was the case in the equilibrium problems considered in [19, 21]. Here we wish to consider a boundary value problem generating inhomogeneous deformation such that the overall volume of the gel increases as some loading parameter increases. In this way, we can consider the transition from saturation to nonsaturation in the context of inhomogeneous deformation. For

[4]By specific threshold volume we mean the threshold volume divided by the polymer volume. It is also important to note that the analogy with incompressible material behavior does not hold for nonsaturated response under inhomogeneous deformation because the local volume may then vary spatially.

this purpose, we consider a cylinder with annular cross section that is first everted and then extended axially.

The simple eversion deformation (turning a cylinder inside-out in such a way that cylindrical surfaces are mapped to cylindrical surfaces) has been studied extensively in hyperelasticity beginning with Rivlin [17]. For the Mooney-Rivlin constitutive law, he found that the simple eversion deformation was not consistent with conditions of zero-traction boundary conditions at the two ends, which motivated him to employ zero end resultant load conditions instead. This is consistent with turning a small piece of rubber tubing inside-out and then letting it go. If the tube remains inside-out upon release, one observes that the ends typically flare out a bit. This indicates that some departure from a simple eversion is necessary to meet a zero traction condition. Varga [22] gives experimental examples for the eversion of different cylinders with free ends, and discusses the extent to which the conditions for a simple eversion deformation are met in the region away from the two ends. Analytical study of the eversion deformation in the context of compressible hyperelasticity is given in [3, 10, 11].

For the eversion of a gel cylinder, the boundary value problem when the cylinder is saturated is formulated as in conventional compressible hyperelasticity. Since we are here dealing with a form for the stored energy density that involves both a Flory-Huggins contribution and a Mooney-Rivlin contribution, one finds that the eversion problem must be solved numerically. As one would anticipate, the numerical solution shows that stretching the cylinder by increasing the axial load causes an increase in the total volume of the everted cylinder. Transition from a saturated condition to a not saturated condition takes place if the amount of fluid for intake into the cylinder is limited. The boundary value problem for a cylinder that is not saturated is formulated with the constraint that the total volume of the cylinder is fixed. This is a global constraint and not a pointwise constraint. As such the associated constraint pressure does not vary spatially. The mathematical character of the boundary value problem does not change significantly after the transition from saturation to nonsaturation. In particular, the governing equations of equilibrium remain the same, since the constraint pressure term in the Cauchy stress is spatially constant and so vanishes upon differentiation. The constraint pressure does however enter into the boundary conditions, and this provides the additional freedom to meet the global volume constraint.

We find that the physical character of the nonsaturated solution to the eversion problem differs from that of the particular saturated solution that would obtain if sufficient fluid had been present. As in the case of homogeneous deformation, it is found that the nonsaturated quasi-static response is inherently stiffer than a continued saturated response. Since the total volume remains fixed after a transition from saturation to nonsaturation, the total fluid content also remains fixed. However it is found that this fixed amount of fluid can redistribute within the everted cylinder as the quasi-static loading proceeds.

2 The Flory-Huggins Equation for the Determination of Free Swelling

The most basic description of large strain effects in elastomeric gels concerns the determination of the amount of fluid that perfuses a polymer matrix when it is placed in a liquid bath. Let ν denote the volume fraction of polymer matrix so that $1 - \nu$ is the volume fraction of the fluid component. A standard development proceeds by taking molecular chain arguments for configurational entropy of crosslinked macromolecules within a liquid bath, and coupling these to a phenomenological description of enthalpy of mixing [18, 20]. The

requirement of a stationary free energy then leads to the equation

$$\underbrace{M\big[\ln(1-\nu_{fs})+\nu_{fs}+\chi\nu_{fs}^2\big]}_{\text{dilution}}+\underbrace{\mu\nu_{fs}^{1/3}}_{\text{crosslinking}}=0 \tag{1}$$

for the equilibrium free-swelling value of ν which, as indicated above, will be denoted by ν_{fs}. Here $M>0$, χ and $\mu>0$ are constitutive parameters that may vary with temperature, pH, fluid chemistry, and other environmental factors. As indicated in (1), two separate effects can be identified, that associated with dilution and that associated with crosslinking. In the absence of crosslinking, the equation reduces to that for the effect of dilution alone, and this is the equation that is usually referred to as the Flory-Huggins equation [20]. The dilution term itself models the two effects of mixing entropy and mixing enthalpy. The term containing χ models the latter and is positive for the standard case wherein polymer–polymer and liquid–liquid grouping is favored over polymer–liquid grouping. In particular, larger χ favors polymer–polymer aggregation so that ν_{fs} increases with χ. The remaining part of the dilution term models the entropy contribution of polymer–liquid mixing to the free energy. In particular, the parameter M is identified as the product of the ideal gas constant and the absolute temperature divided by the molar volume of the liquid.

The utility of a theory that delivers (1) is due in no small part to the fact that (1) *has a unique solution* ν_{fs} *that takes values on the physically relevant interval* $0<\nu_{fs}<1$. This solution is here referred to as the *free swelling polymer volume fraction*. It is completely determined by χ and the ratio μ/M. Thus one may then write $\nu_{fs}=\hat{\nu}_{fs}(\chi,\mu/M)$. Increasing either χ or μ/M favors a more tightly bound gel and so increases $\hat{\nu}_{fs}(\chi,\mu/M)$.

Additional thermodynamic quantities that are then derived from this framework, such as the relative vapor pressure of the liquid swelling agent [20], show good agreement with experiment and so validate the basic soundness of the theoretical assumptions. It must however be remembered that the specific functional form in (1) is the result of geometrical and statistical arguments involving crosslinked macromolecular chains. For example, as is evident from the development given by Doi [4], the term in (1) that arises from configurational entropy considerations, i.e. $M(\ln(1-\nu_{fs})+\nu_{fs})$, is ultimately based on a counting argument which is itself simplified by neglecting certain terms that can be regarded as small so long as the polymer is composed of very many chain segments. Similarly, the term arising from crosslinking, $\mu\nu_{fs}^{1/3}$, involves assumptions on the geometry and statistics of the crosslink network. Different assumptions with regard to microstructural effects (the nature of the crosslinking, the interaction enthalpy, the overall chain extensibility, etc.) or different analysis of the microstructural effects (self-avoiding chains, etc.) would in general lead to modification of (1). Nevertheless the basic idea remains, energy minimization determines the free swelling volume fraction so that the specific form of the energy to be minimized is the central ingredient in the description. The situation is analogous to that of conventional hyperelasticity wherein a well known microstructural argument makes plausible the neo-Hookean strain energy density function (viz. [20]), whereas different arguments lead to other forms, all of which can be used to analyze the deformation of rubbery materials.

The connection between free swelling and hyperelasticity follows by introducing the deformation mapping that takes the polymer component from its original unswollen location $\mathbf{X}$ to its stressed, swollen location $\mathbf{y}$. Let $J=\det\mathbf{F}$ where $\mathbf{F}=\partial\mathbf{y}/\partial\mathbf{X}$ is the deformation gradient of the mapping $\mathbf{y}(\mathbf{X})$. Correspondence between J and ν is immediate if both the polymer component and the fluid component are individually incompressible since simple mixing then gives the identification $J=1/\nu$. Thus J is the volumetric swelling of the gel as

measured with respect to the polymer component before liquid was present. It is therefore required that

$$J \geq 1. \tag{2}$$

Historically, the original development leading to (1) employed a notion of physical variations. In particular, rather than using physical arguments to obtain an explicit energy to minimize, the original papers of Flory and Treloar employ an argument which requires that there is no change in the free energy of the system in the event that a single fluid particle is transfered between the gel and the pure liquid which surrounds the gel. Although the free swelling volume fraction appears in (1), the original arguments leading to this equation actually depend more on the concept of occupied volume rather than the related concept of volume fraction. The connection between occupied volume and volume fraction then follows from $J = 1/\nu$. The argument involving fluid particle transfer can thus be viewed as a variation with respect to J. Accordingly, the energy that is formally minimized can be found by substituting $\nu_{fs} \to 1/J$ in (1), integrating the resulting expression with respect to J, and, if desired, returning to the original volume fraction variable via $J \to 1/\nu_{fs}$. Hence (1) is equivalent to determining the free-swelling value of J as the root of

$$\frac{d}{dJ}\big(H(J) + \Psi(J)\big) = 0, \tag{3}$$

with

$$H(J) = M\big((J-1)\ln(1-J^{-1}) + \chi(1-J^{-1})\big), \tag{4}$$

and

$$\Psi(J) = \frac{3\mu}{2}J^{2/3}. \tag{5}$$

Here $H + \Psi$ is the overall free energy, the former accounting for polymer-fluid interaction (mixing entropy and mixing enthalpy), the latter accounting for elastomeric deformation of the crosslinking network. The limiting case $\mu \to 0$ corresponds to the absence of crosslinking and hence no elastic effect. Equation (3) then reduces to $h(J) = 0$ where we have introduced the notation

$$h(J) \equiv \frac{\partial H}{\partial J}. \tag{6}$$

It is to be remarked that (2) and (3) can be regarded as a general framework, which retrieves the well known equation (1) once the specific mathematical forms (4) and (5) are invoked. Thus statements involving the functions H and Ψ need not be tied to (4) and (5) unless specifically indicated. Similarly, (6) is a definition for h that is not tied to any constitutive form. For the specific constitutive function (4), h is given by

$$h(J) = M\big[\ln(1-J^{-1}) + J^{-1} + \chi J^{-2}\big]. \tag{7}$$

The basic behavior of this framework with the usual forms (4) and (5) is sensitive to whether $\chi < 1/2$ or $\chi > 1/2$ as described next.

If (4) and (5) hold and $\chi > 0.5$ then there is a unique value of $J > 1$ that causes h to vanish. This value of J corresponds to free swelling in the absence of crosslinking and we denote this value by J_{ncl} where the subscript refers to no crosslinking. Thus $h(J_{ncl}) = 0$ and $J_{ncl} = 1/\hat{\nu}_{fs}(\chi, 0)$. Moreover $h(J) < 0$ for $1 < J < J_{ncl}$ and $h(J) > 0$ for $J > J_{ncl}$.

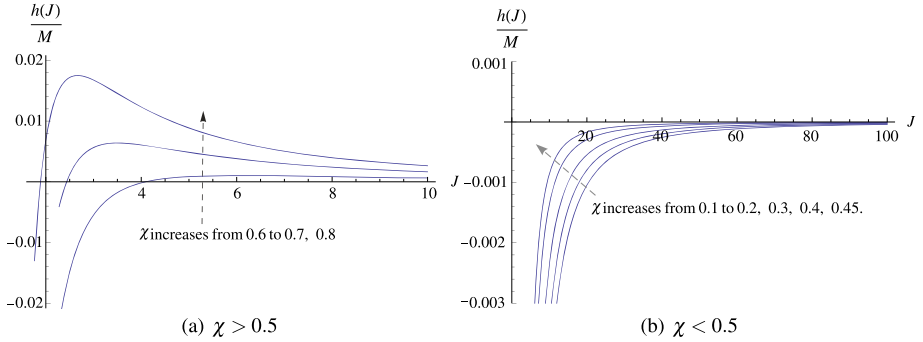

Fig. 1 The constitutive function $h(J)$ in (7) for various χ. Vaues of J giving $h(J) = 0$ model gel dilation on the basis of mixing entropy and mixing enthalpy, but do not account for the elastic effect of polymer crosslinking

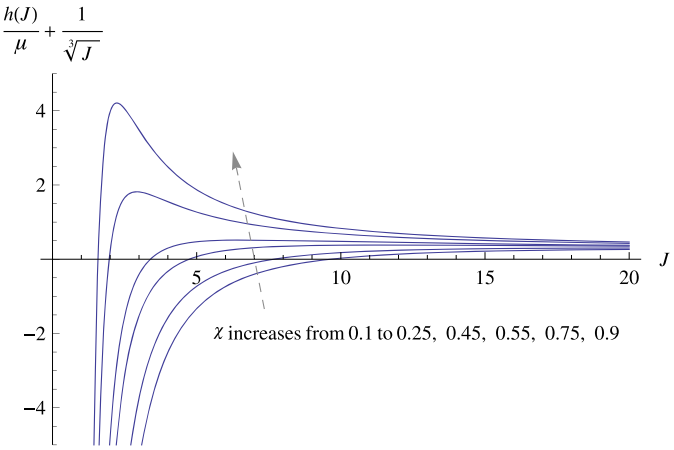

Fig. 2 The constitutive expression $h(J) + \mu J^{-1/3}$ for various χ when $\mu = 0.01M$. The new term $\mu J^{-1/3}$ describes the effect of crosslinks. Values of J giving $h(J) + \mu J^{-1/3} = 0$ describe free swelling

Consequently J_{ncl} provides a local minima of H. One also finds that $J_{ncl} < 2\chi/(2\chi - 1)$ and that $J_{ncl} \to \infty$ as $\chi \to 0.5$.

If (4) and (5) hold and $\chi < 0.5$ then there are no solutions to $h(J) = 0$ because $h(J) < 0$ for all $J > 1$. Hence for $\chi < 0.5$ the infimum of H is achieved as $J \to \infty$. Since $h(J) \to 0$ as $J \to \infty$ it is convenient to formally define $J_{ncl} \equiv \infty$ for $\chi < 0.5$. The derivative $h'(J) > 0$ for all $J > 1$. These qualitative features are summarized in Fig. 1.

Accounting for elastic interconnection ($\mu > 0$), (3)–(5) become $h(J) + \mu J^{-1/3} = 0$. In conjunction with (7) this recovers (1) for the free swelling value $J_{fs} \equiv 1/v_{fs}$. There is a unique finite J_{fs} solution to (3)–(5) for all χ whenever $\mu > 0$, which is formally given by $J_{fs} = 1/\hat{v}_{fs}(\chi, \mu/M)$. This solution obeys the inequality $J_{fs} < J_{ncl}$ as would be expected since the crosslinking inhibits swelling. Further $h(J) + \mu J^{-1/3}$ is respectively positive or negative as J is respectively greater than or less than J_{fs}. Figure 2 indicates these relations.

A simple interpretation concerns polymer that has some original volume, say V_p, when free of liquid. Placing this nominally dry polymer into a liquid bath causes it to swell by uptake of fluid. The resulting gel occupies new volume JV_p where J minimizes the free

energy $H(J)+\Psi(J)$. For the energy forms (4) and (5) this free energy involves the three previously mentioned effects, one of which favors swelling (the configurational entropy), one of which opposes it (crosslinking), and one of which could go either way (mixing enthalpy) although it opposes swelling in the standard case $\chi > 0$. In all cases, crosslinking ($\mu > 0$) ensures that the swollen volume remains finite. If crosslinks are not present ($\mu = 0$) then the mixing enthalpy must sufficiently favor same phase agglomeration ($\chi > 0.5$) for the swollen volume to remain finite. However if crosslinking is not present and the mixture enthalpy is not sufficiently conducive to this same phase agglomeration ($\mu = 0$ and $\chi < 0.5$) then $J \to \infty$ and the polymer goes into solution, dispersing itself throughout the fluid bath.

Implicit in the above discussion is a requirement that sufficient liquid is available for saturation of polymer with the liquid. This requires that

$$JV_p \le V_p + V_f, \tag{8}$$

where V_f is the original fluid volume prior to introduction of polymer. If (8) holds then the gel swells to its energetically favored saturation value. However if J as determined on the basis of (3) is larger than that permitted by (8) then the swelling is limited by the availability of fluid to the value

$$J_* \equiv 1 + V_f/V_p \tag{9}$$

which is less than the free swelling value J_{fs} determined on the basis of (3). The gel is then no longer saturated. In what follows the use of a subscript $_*$ or a superscript * will denote a value that demarcates a transition between saturation and nonsaturation.

3 Hyperelastic Constitutive Theory

In free swelling, the deformation gradient of the mapping $\mathbf{y}(\mathbf{X})$ is $\mathbf{F} = J_{fs}^{1/3}\mathbf{I}$ where $\mathbf{I}$ is the identity tensor. In order to treat more general deformations due to the effect of mechanical loading, we now consider a hyperelastic framework. Let $\mathbf{B} = \mathbf{F}\mathbf{F}^T$ and $\mathbf{C} = \mathbf{F}^T\mathbf{F}$ and let I_1, I_2 and I_3 be the associated principal scalar invariants

$$I_1 = \text{Trace}\,\mathbf{B}, \qquad I_2 = \frac{1}{2}(I_1^2 - \text{Trace}(\mathbf{B}^2)), \qquad I_3 = \det\mathbf{B} = J^2.$$

The overall stored energy density will be expressed as the sum of elastic free energy of the polymer network Φ and a mixing free energy H

$$W(\mathbf{F}) = \Phi(I_1, I_2, J) + H(J). \tag{10}$$

The mixing energy H is the same as that discussed in the previous section and its derivative will continue to be denoted by h (viz. (6)). The specific Flory-Huggins form (4) for H will be used in the examples that follow.

3.1 Free Swelling

In the absence of mechanical loading, the associated free swelling is determined by minimizing W in the class of simple volumetric expansions $\mathbf{F} = J^{1/3}\mathbf{I}$ so that $I_1 = 3J^{2/3}$ and $I_2 = 3J^{4/3}$. Thus J is determined on the basis of

$$\frac{d}{dJ}\big(\Phi(3J^{2/3}, 3J^{4/3}, J) + H(J)\big) = 0.$$

Comparison with (3) indicates that correspondence with the free swelling framework described in the previous section will follow provided that

$$\Phi(3J^{2/3}, 3J^{4/3}, J) = \Psi(J) + \text{constant}.$$

Correspondence with the particular Flory-Huggins form (5) will obtain if

$$\Phi(3J^{2/3}, 3J^{4/3}, J) = \frac{3\mu}{2} J^{2/3} + \text{constant}.$$

In what follows we shall use the Mooney-Rivlin form for the elastic energy Φ of the polymer network

$$\Phi = \Phi(I_1, I_2) = \frac{\mu}{2}\big[(1-\xi)(I_1-3) + \xi(I_2-3)\big], \quad (0 \le \xi \le 1). \tag{11}$$

The case $\xi = 0$ gives the neo-Hookean specialization. For any ξ obeying $0 \le \xi \le 1$ in (11), one finds that

$$\Phi(3J^{2/3}, 3J^{4/3}, J) = \frac{3\mu}{2}\big((1-\xi)J^{2/3} + \xi J^{4/3} - 1\big)$$

so that the special neo-Hookean case of $\xi = 0$ retrieves the original equation (1) upon taking $J = J_{fs} = 1/\nu_{fs}$. For the more general Mooney-Rivlin form with $\xi > 0$ equation (1) is augmented so as to contain an additional term and so becomes

$$M\big[\ln(1-\nu_{fs}) + \nu_{fs} + \chi\nu_{fs}^2\big] + \mu\big[(1-\xi)\nu_{fs}^{1/3} + 2\xi\nu_{fs}^{-1/3}\big] = 0. \tag{12}$$

Introduce the free swelling stretch ratio

$$\zeta \equiv J_{fs}^{1/3} = \nu_{fs}^{-1/3}, \tag{13}$$

where ν_{fs} is the root of (12). This root now depends upon ξ in addition to χ and μ/M. As such, the free swelling behavior under (12) is not as simply described as was the case for (1). Some indication of the effect of the new constitutive parameter ξ upon ν_{fs} can be obtained by taking representative values for χ and μ/M. To this end we follow [23] where the equivalent of a neo-Hookean Φ is considered for the modeling of a vulcanized rubber in contact with toluene as considered by Paul and Ebra-Lima in [13]. The following values are taken in [23]: $M = 2.379 \times 10^8$ dyne/cm^2, $\chi = 0.425$ and $\mu = 2.375 \times 10^6$ dyne/cm^2. Note for these values that the dimensionless parameter $\bar{M} = M/\mu = 100.17 \approx 100$. The value of the free swelling stretch ratio ζ as a function of ξ for various $\bar{M}$ and χ are shown in Fig. 3. The dotted curves in Fig. 3(a) and Fig. 3(b) are respectively associated with the above parameters $\bar{M} = 100$ and $\chi = 0.425$.

3.2 Stress

Let $\mathbf{T}$ and $\boldsymbol{\sigma}$ give the first Piola-Kirchhoff and Cauchy stress tensors, respectively. They are connected by

$$\boldsymbol{\sigma} = \frac{1}{J}\mathbf{T}\mathbf{F}^T. \tag{14}$$

Mechanical equilibrium is governed by the usual equations

$$\text{Div}\,\mathbf{T} = \mathbf{0} \quad \text{on } \Omega_{\mathbf{X}} \quad \Leftrightarrow \quad \text{div}\,\boldsymbol{\sigma} = \mathbf{0} \quad \text{on } \Omega_{\mathbf{y}}, \tag{15}$$

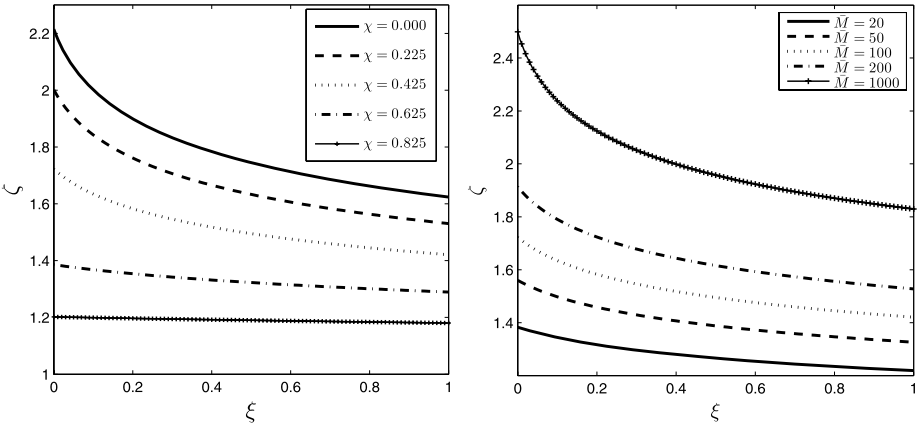

(a) $\bar{M} = 100$ and χ varying from 0.000 to 0.825 (b) $\chi = 0.425$ and $\bar{M}$ varying from 20 to 1000

Fig. 3 The free swelling stretch ratio ζ as given by (12) and (13) is a function of $\bar{M}$, χ and ξ. The dependence of ζ on ξ is shown for various $\bar{M}$ and various χ

where $\Omega_{\mathbf{X}}$ and $\Omega_{\mathbf{y}}$ denote the gel domain in the reference and deformed configuration, respectively. We continue to let V_p and V_f be the volume of polymer and fluid respectively. In particular

$$V_p = \int_{\Omega_{\mathbf{X}}} dV_{\mathbf{X}}. \tag{16}$$

After mixing the local gel volume is J so that the overall gel volume is

$$V \equiv \int_{\Omega_{\mathbf{X}}} J\, dV_{\mathbf{X}}. \tag{17}$$

The maximum overall gel volume is $V_p + V_f$ corresponding to uptake of all fluid into the gel. So long as this does not occur the gel is able to saturate. The system is not saturated only if $V = V_p + V_f$. Together this gives the global constraint

$$\int_{\Omega_{\mathbf{X}}} (J-1)\, dV_{\mathbf{X}} \leq V_f. \tag{18}$$

If the system is saturated then the first Piola-Kirchhoff stress tensor is given by $\mathbf{T} = \partial W/\partial \mathbf{F}$ and the saturated Cauchy stress tensor is

$$\boldsymbol{\sigma} = \frac{2}{J}\mathbf{F}\frac{\partial \Phi}{\partial \mathbf{C}}\mathbf{F}^T + h(J)\mathbf{I}, \quad \text{(saturated)}, \tag{19}$$

where the first term on the right hand side follows exactly as from conventional hyperelasticity and the second term on the right hand side follows upon recalling that $\partial J/\partial \mathbf{F} = J\mathbf{F}^{-T}$.

If, however, the material is not saturated, then a constant reaction stress $-p\mathbf{I}$ is generated so as to enforce the constraint (18). This gives the nonsaturated Cauchy stress tensor

$$\boldsymbol{\sigma} = \frac{2}{J}\mathbf{F}\frac{\partial \Phi}{\partial \mathbf{C}}\mathbf{F}^T + h(J)\mathbf{I} - p\mathbf{I}, \quad \text{(not saturated)}. \tag{20}$$

Thus, as in incompressible hyperelasticity, there is a pressure contribution to the Cauchy stress tensor that is not determined by the deformation.

Here, however, it is important to emphasize that the constraint (18) is a global one. This is in contrast to the situation in conventional incompressible hyperelasticity in which the constraint $\det \mathbf{F} = 1$ is a local one. The pointwise constraint in incompressible hyperelasticity gives rise to a reactive pressure that can vary spatially. In contrast, the pressure p in (20) takes the same value at every point in the nonsaturated gel. In particular, since p in (20) is constant, a condition of spatially varying J does not generally permit the last two terms in (20) to be consolidated into a single term with redefined p.

Evaluating $\partial\Psi/\partial\mathbf{C}$ in terms of the dependence on I_1, I_2, J gives

$$\boldsymbol{\sigma} = -\frac{2}{J}\frac{\partial \Phi}{\partial I_2}\mathbf{B}^2 + \frac{2}{J}\left(\frac{\partial \Phi}{\partial I_1} + I_1\frac{\partial \Phi}{\partial I_2}\right)\mathbf{B} + \left(\frac{\partial \Phi}{\partial J} + h(J)\right)\mathbf{I}, \quad \text{(saturated)}, \tag{21}$$

while the nonsaturated Cauchy stress tensor becomes

$$\boldsymbol{\sigma} = -\frac{2}{J}\frac{\partial \Phi}{\partial I_2}\mathbf{B}^2 + \frac{2}{J}\left(\frac{\partial \Phi}{\partial I_1} + I_1\frac{\partial \Phi}{\partial I_2}\right)\mathbf{B} + \left(\frac{\partial \Phi}{\partial J} + h(J) - p\right)\mathbf{I}, \quad \text{(not saturated)}. \tag{22}$$

4 Homogeneous Deformation Response

We now consider the homogeneous deformation response using the constitutive forms (11) and (4) in (10). Since J is a constant for homogeneous deformation, condition (18) reduces to the same condition as in free swelling, namely (8). This in turn is equivalent to the condition $J \le J_*$ where J_* is defined in (9). The Cauchy stress tensor then follows from (21) and (22) as

$$\boldsymbol{\sigma} = \frac{\mu}{J}[(1 - \xi + \xi I_1)\mathbf{B} - \xi\mathbf{B}^2] + h(J)\mathbf{I}, \quad (1 \le J < J_*), \tag{23}$$

$$\boldsymbol{\sigma} = \frac{\mu}{J_*}[(1 - \xi + \xi I_1)\mathbf{B} - \xi\mathbf{B}^2] + (h(J_*) - p)\mathbf{I}, \quad (J = J_*). \tag{24}$$

Since the term $(h(J_*) - p)$ in (24) involves constant $h(J_*)$ and an arbitrary constant p, it follows that $h(J_*)$ can be absorbed into p. However later, when inhomogeneous deformation is considered, it will be necessary to retain $h(J)$ in the nonsaturated Cauchy stress tensor.

We now consider in turn: equibiaxial loading, uniaxial loading, and equitriaxial loading. Each is referred to a coordinate system with mutually orthogonal unit vectors $\mathbf{e}_1, \mathbf{e}_2, \mathbf{e}_3$.

4.1 Equibiaxial Stress

This is the specialization $\boldsymbol{\sigma} = \sigma(\mathbf{e}_1 \otimes \mathbf{e}_1 + \mathbf{e}_2 \otimes \mathbf{e}_2)$ and we restrict attention to deformations that preserve the loading symmetry so that $\mathbf{F} = \lambda(\mathbf{e}_1 \otimes \mathbf{e}_1 + \mathbf{e}_2 \otimes \mathbf{e}_2) + (J/\lambda^2)\mathbf{e}_3 \otimes \mathbf{e}_3$. For a saturated material it follows from (23) that

$$\mu\left[\frac{\lambda^2}{J} + \xi\left(\frac{\lambda^2}{J}(\lambda^2 - 1) + \frac{J}{\lambda^2}\right)\right] + h(J) = \sigma, \quad \text{(saturated)}, \tag{25}$$

and

$$\mu\left[\frac{J}{\lambda^4} + \xi\left(\frac{J}{\lambda^4}(2\lambda^2 - 1)\right)\right] + h(J) = 0, \quad \text{(saturated)}. \tag{26}$$

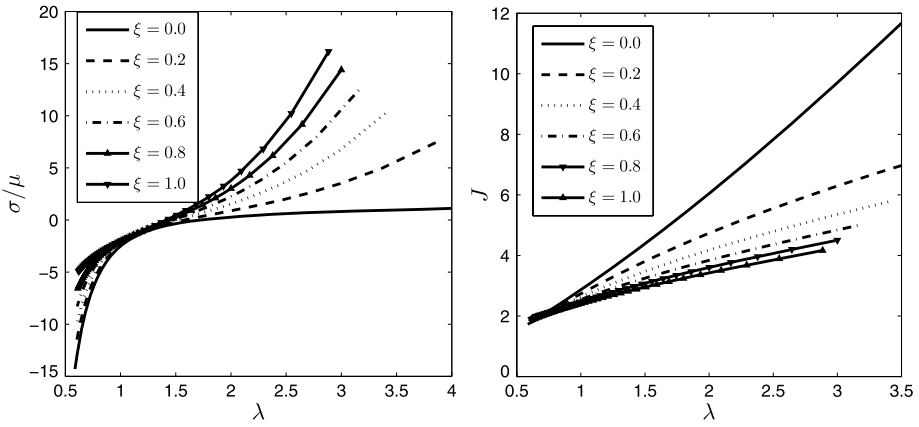

(a) σ/μ versus λ for equibiaxial loading (b) J versus λ for equibiaxial loading

Fig. 4 Stress–stretch behavior and volume–stretch behavior for equibiaxial loading of a saturated gel with $\bar{M} = 100$ and $\chi = 0.425$ showing the effect of different ξ

The second equation provides the relation between J and λ whereupon the first equation provides σ in terms of either λ or J. The graph of stress vs. stretch passes through the point $(\lambda, \sigma) = (\zeta, 0)$ which corresponds to the state of free swelling. Recalling the requirement that $J \geq 1$ consider the limit $J \to 1$ in (25) and (26). For h in (26) given by (7) this limit gives

$$\lambda \sim \begin{cases} (-\frac{M}{\mu(1-\xi)} \ln(1 - J^{-1}))^{-1/4}, & \text{if } 0 \leq \xi < 1, \\ (-\frac{M}{2\mu} \ln(1 - J^{-1}))^{-1/2}, & \text{if } \xi = 1, \end{cases} \tag{27}$$

so that, in all cases, $J \to 1$ as $\lambda \to 0$. According to (25) this requires $\sigma \to -\infty$ as follows:

$$\sigma \sim h(J) \sim M \ln(1 - J^{-1}) \sim \begin{cases} -\mu(1-\xi)\lambda^{-4}, & \text{if } 0 \leq \xi < 1, \\ -2\mu\lambda^{-2}, & \text{if } \xi = 1. \end{cases} \tag{28}$$

Thus the limit $\sigma \to -\infty$ forces all of the liquid out of the gel, and in this limit $\lambda \to 0$.

Returning to the overall stress behavior, we find for $M = 100\mu$ and $\chi = 0.425$ that J is monotone in λ for all $0 \leq \xi \leq 1$. The graph of σ vs. λ is also found to be monotone for these parameters (Fig. 4). Thus increasing stretch corresponds to both increasing stress and increasing fluid content. This situation holds so long as $J < J_*$.

A transition from a state of saturation to a state of nonsaturation occurs when $J = J_*$. This occurs at a unique value of λ, say λ^*_{eqbi}, and a unique value of stress, say σ^*_{eqbi}. For $\lambda \geq \lambda^*_{eqbi}$ the value of J remains fixed at J_* and the relation between stress and stretch is now determined on the basis of (24). This gives $\mathbf{F} = \lambda(\mathbf{e}_1 \otimes \hat{\mathbf{e}}_1 + \mathbf{e}_2 \otimes \mathbf{e}_2) + (J_*/\lambda^2)\mathbf{e}_3 \otimes \mathbf{e}_3$ and

$$\sigma = \mu\left[(1-\xi)\left(\frac{\lambda^2}{J_*} - \frac{J_*}{\lambda^4}\right) + \xi\left(\frac{\lambda^4}{J_*} - \frac{J_*}{\lambda^2}\right)\right], \quad \text{(not saturated)}. \tag{29}$$

It is to be remarked that the nonsaturated response does not depend upon $h(J)$.

The solid curve in Fig. 5 shows the saturated backbone curve σ vs. λ for $\xi = 0$. The transition stretch λ^*_{eqbi} can take on any value as determined by J_*, and three values of λ^*_{eqbi} are taken as examples. At each such λ^*_{eqbi} there is a transition from saturated to nonsaturated

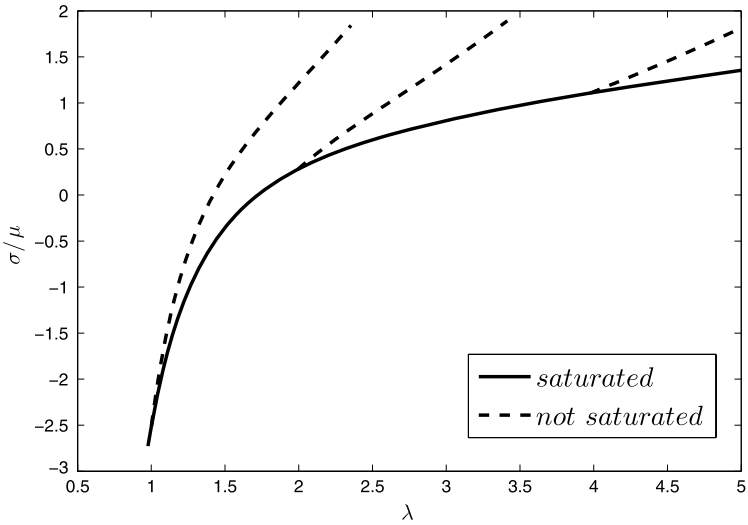

Fig. 5 Stress–stretch behavior for equibiaxial loading with $\bar{M} = 100$, $\chi = 0.425$, and $\xi = 0$. Three nonsaturated response curves are depicted. Each nonsaturated response branches off of the saturated response "backbone curve"

response, and the associated nonsaturated response curve that branches off of the backbone curve does so in a continuous but nonsmooth fashion. The nonsaturated response involves an abrupt stiffening as evidenced by the greater slope of the nonsaturated curve at the branch point. To be specific, suppose $\lambda \geq \lambda^*_{eqbi}$ so that the gel is not saturated because insufficient liquid is available. Consider the difference in the value of stress for the nonsaturated response and the value of stress for a hypothetical saturated response had sufficient liquid been available. This difference is

$$\sigma_{non} - \sigma_{sat} = \left[\mu(1-\xi)\lambda^2\left(\frac{1}{J_*} - \frac{1}{J}\right)\right] + \left[\frac{\mu(1-\xi)}{\lambda^4}(J - J_*)\right] + \left[\mu\xi\lambda^4\left(\frac{1}{J_*} - \frac{1}{J}\right)\right] + \left[\frac{\mu\xi}{\lambda^2}(J - J_*)\right], \tag{30}$$

where J in the above expression is the saturation value. Since $J > J_*$ if $\lambda > \lambda^*_{eqbi}$ it follows that each of the four separate bracketed terms in the above expression is positive after loss of saturation. One therefore formally verifies that $\sigma_{non} > \sigma_{sat}$ if $\lambda > \lambda^*_{eqbi}$. In addition, by differentiating the expression in (30) with respect to λ and then evaluating the result at $\lambda = \lambda^*_{eqbi}$ and $J = J_*$, one obtains the slope difference at the location where a nonsaturated response curve branches off of the saturation response curve. This calculation gives

$$\left.\frac{d}{d\lambda}(\sigma_{non} - \sigma_{sat})\right|_{\lambda=\lambda^*_{eqbi}} = \mu\left[(1-\xi)\left(\frac{\lambda^2}{J_*^2} + \frac{1}{\lambda^4}\right) + \xi\left(\frac{\lambda^4}{J_*^2} + \frac{1}{\lambda^2}\right)\right]\Bigg|_{\lambda=\lambda^*_{eqbi}} \left.\frac{dJ}{d\lambda}\right|_{\lambda=\lambda^*_{eqbi}}. \tag{31}$$

Noting that the bracketed term in the above expression is positive, it follows that the sign of the above expression is determined by the sign of the derivative $dJ/d\lambda$. Since, as remarked above, J increases with λ it follows that the slope difference is strictly positive, thus quantifying the abrupt stiffening.

Returning to Fig. 5 it is observed that two of the three nonsaturated response curves depicted in this figure involve values of J_* that give $\sigma^*_{eqbi} > 0$. For these two J_* there is sufficient liquid for free swelling and the resulting loss of saturation occurs once σ increases to $\sigma^*_{eqbi} > 0$. The third nonsaturated response curve depicted in Fig. 5 involves a value J_* that gives $\sigma^*_{eqbi} < 0$. In this case there is insufficient liquid for free swelling to proceed to its saturated value. Thus the value $\sigma = 0$ occurs on a nonsaturated response curve. A biaxial compressive stress will, in this case, give a response that proceeds down the nonsaturated curve until it joins the saturated backbone curve. The resulting transition from nonsaturated to saturated response now involves an abrupt softening in the Cauchy stress response.

4.2 Uniaxial Stress

This is the specialization $\boldsymbol{\sigma} = \sigma \mathbf{e}_1 \otimes \mathbf{e}_1$ and we again restrict attention to deformations that preserve the loading symmetry so that $\mathbf{F} = \lambda \mathbf{e}_1 \otimes \mathbf{e}_1 + \sqrt{J/\lambda}(\mathbf{e}_2 \otimes \mathbf{e}_2 + \mathbf{e}_3 \otimes \mathbf{e}_3)$. For a saturated gel it follows from (23) that

$$\mu\left[(1-\xi)\frac{\lambda^2}{J} + 2\xi\lambda\right] + h(J) = \sigma, \quad \text{(saturated)}, \tag{32}$$

and

$$\mu\left[(1-\xi)\frac{1}{\lambda} + \xi\left(\lambda + \frac{J}{\lambda^2}\right)\right] + h(J) = 0, \quad \text{(saturated)}. \tag{33}$$

The latter provides the kinematic relation between J and λ (Fig. 6b) while the former then gives the relation between uniaxial stress σ and stretch ratio λ (Fig. 6a). The graph of stress vs. stretch again passes through the free swelling point $(\lambda, \sigma) = (\zeta, 0)$. The predicted behavior associated with the possibility of squeezing out all of the liquid in uniaxial stress again requires the consideration of $J \to 1$. For h given by (7) it is again found that $\lambda \to 0$ as $J \to 1$. In particular, one finds that $\lambda \sim O([\ln((J-1)^{-1})]^{-1/2})$ if $0 < \xi \leq 1$, while $\lambda \sim O([\ln((J-1)^{-1})]^{-1})$ if $\xi = 0$. In all cases $\sigma \to -\infty$ as $\lambda \to 0$. As regards the overall stress behavior, we find that σ is monotonically increasing with λ when $M = 100\mu$ and $\chi = 0.425$ for all $0 \leq \xi \leq 1$.

For $\xi = 0$ it is found that the volume increases monotonically with axial stretch (viz. Fig. 6b). Thus, as in the case of equibiaxial stress, there will be a loss of saturation when $J = J_*$. The stress vs. stretch response must then be determined using (24). This gives

$$\sigma = \mu\left(\frac{\lambda^2}{J_*} - \frac{1}{\lambda}\right)\left(1 - \xi + \xi\frac{J_*}{\lambda}\right), \quad \text{(not saturated)}. \tag{34}$$

Even though we are currently considering the case $\xi = 0$ we have, for the sake of later discussion, given the more general expression in the above equation. Returning again to the case $\xi = 0$, the associated nonsaturated response curve can again be regarded as branching off of the backbone saturated response curve. As shown in Fig. 7, each nonsaturated response curve is well separated from the backbone curve. Indeed as $\lambda \to \infty$ the $\xi = 0$ specialization of (32) and (33) give

$$J \sim \left(\bar{M}\left(\frac{1}{2} - \chi\right)\right)^{1/2}\lambda^{1/2} + \frac{1}{3-6\chi} + O(\lambda^{-1/2}), \quad (\xi = 0, \text{ saturated}), \tag{35}$$

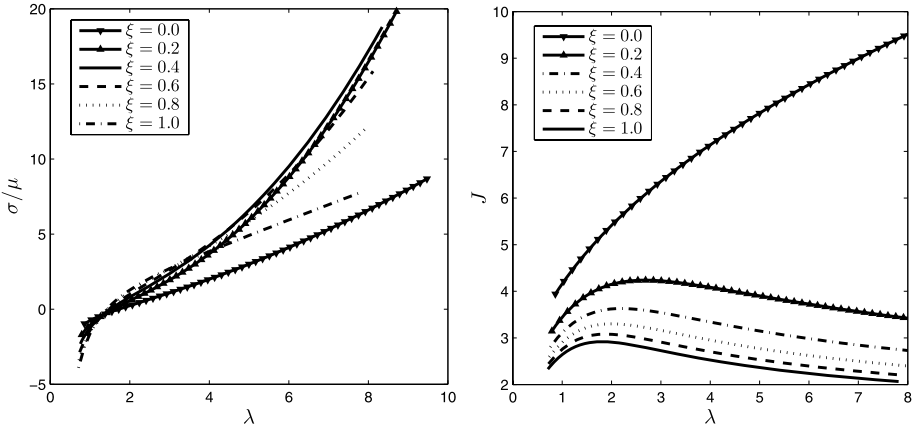

(a) σ/μ versus λ (b) J versus λ

Fig. 6 Stress–stretch behavior and volume–stretch behavior for uniaxial loading of a saturated gel with $\bar{M} = 100$ and $\chi = 0.425$ showing the effect of different ξ

and

$$\sigma \sim \frac{\mu}{(\bar{M}(\frac{1}{2} - \chi))^{1/2}}\lambda^{3/2} - \frac{2}{3\bar{M}(1-2\chi)^2}\lambda + O(\lambda^{1/2}), \quad (\xi = 0, \text{ saturated}). \tag{36}$$

Specifically, the Cauchy stress for the saturated gel is $O(\lambda^{3/2})$ as $\lambda \to \infty$. In contrast, (34) indicates that the Cauchy stress for the nonsaturated gel is $O(\lambda^2)$, which accounts for the increasing separation between the response curves in Fig. 7.

It is useful to note that the separation between the saturated and nonsaturated stress response for the $\xi = 0$ gel is not present in the corresponding first Piola-Kirchhoff stress. Recalling (14) it follows that this stress is $\mathbf{T} = T\mathbf{e}_1 \otimes \mathbf{e}_1$ with $T = \sigma J/\lambda$. It then follows from (32) and (33) that the large stretch Piola-Kirchhoff stress response of the saturated $\xi = 0$ gel is

$$T \sim \mu\lambda - \mu\left(\bar{M}\left(\frac{1}{2} - \chi\right)\right)^{1/2}\lambda^{-3/2} + O(\lambda^{-2}), \quad (\xi = 0, \text{ saturated}). \tag{37}$$

Turning to the first Piola-Kirchhoff stress response of a $\xi = 0$ gel that is not saturated, it is immediate from (34) that

$$T = \mu\lambda - \mu\frac{J_*}{\lambda^2}, \quad (\xi = 0, \text{ not saturated}). \tag{38}$$

Thus the saturated and nonsaturated Piola-Kirchhoff stress response have the same leading order behavior as $\lambda \to \infty$. Moreover, the separation between the saturated and nonsaturated Piola-Kirchhoff stress response curves is $O(\lambda^{-3/2})$ as the stretch increases, and hence vanishingly small. Since first Piola-Kirchhoff stress directly scales with applied load in a standard testing device, it follows that such a testing device may have difficulty distinguishing between saturated response and nonsaturated response.

The situation is even more complicated for $0 < \xi \leq 1$ since we find for this case that J exhibits a local maximum, say J_{max}, at a finite value of uniaxial stretch. If $J_{max} < J_*$ then

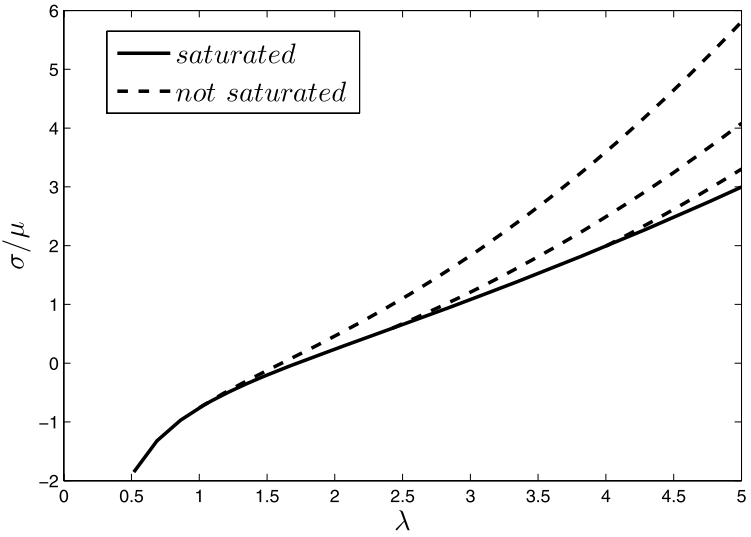

Fig. 7 Stress–stretch behavior for uniaxial loading with $\bar{M} = 100$, $\chi = 0.425$, and $\xi = 0$. Three nonsaturated response curves are depicted

there is always sufficient liquid for the gel to remain saturated. However if $J_{max} > J_*$ then the saturation value of J will be greater than J_* on a finite interval of stretch, say $\lambda^*_{uni-A} < \lambda < \lambda^*_{uni-B}$ where the endpoint values λ^*_{uni-A}, λ^*_{uni-B} correspond to $J = J_*$ in uniaxial loading. On this interval the nonsaturated response is given by (34). The nonsaturated response curve therefore branches off of the backbone curve at λ^*_{uni-A} and rejoins the backbone curve at λ^*_{uni-B}. This is shown in Fig. 8, where it is to be remarked that the separation between the $\xi = 1$ saturated and nonsaturated stress response is difficult to distinguish (unlike the $\xi = 0$ case shown in Fig. 7).

By a development parallel to that giving (30) one may show that any nonsaturated uniaxial response curve is above the backbone saturated uniaxial response curve. The change in slope where a nonsaturated response curve connects to a saturated response curve can also be found by the type of development that led to (31) for the equibiaxial case. The corresponding result for uniaxial stress is

$$\frac{d}{d\lambda}(\sigma_{non} - \sigma_{sat})\bigg|_{\lambda=\lambda^*_{uni}} = \mu\left[(1-\xi)\frac{\lambda^2}{J_*} + \frac{\xi}{\lambda^2}\right]\bigg|_{\lambda=\lambda^*_{uni}} \frac{dJ}{d\lambda}\bigg|_{\lambda=\lambda^*_{uni}}. \tag{39}$$

The sign of this expression is again determined by the derivative term $dJ/d\lambda$. This derivative is positive at λ^*_{uni-A} and negative at λ^*_{uni-B}. Thus, under increasing stretch, an abrupt stiffening occurs in the Cauchy stress for both the loss of saturation transition at λ^*_{uni-A} and for the regain of saturation transition at λ^*_{uni-B}.

4.3 Equitriaxial Stress

This is the specialization $\boldsymbol{\sigma} = \sigma\mathbf{I}$ with $\mathbf{F} = J^{1/3}\mathbf{I}$. The relation between σ and J then follows from (23 and (7) as

$$\sigma = \mu\big[(1-\xi)J^{-1/3} + 2\xi J^{1/3}\big] + M\big[J^{-1} + \chi J^{-2} + \ln(1-J^{-1})\big]. \tag{40}$$

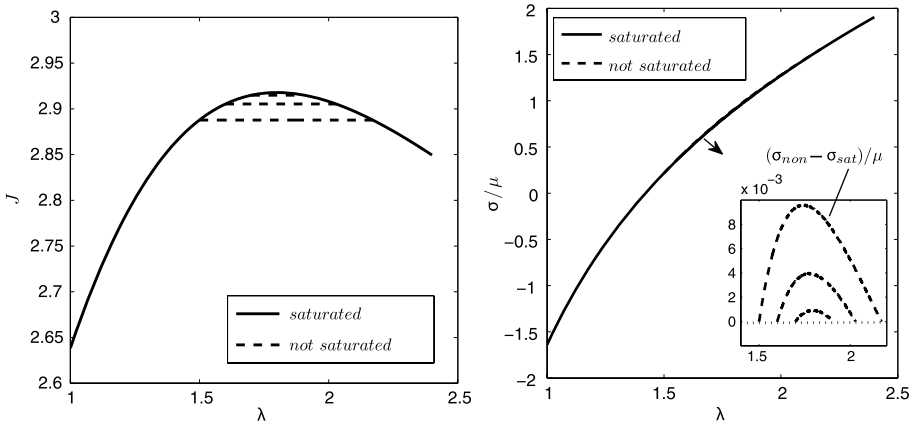

(a) J versus λ (b) σ/μ versus λ

Fig. 8 The dependence of volume and stress on uniaxial stretch for $\bar{M} = 100$, $\chi = 0.425$, and $\xi = 1$. Three nonsaturated examples are shown corresponding to loss of saturation at $\lambda^*_{uni-A} = 1.5$, 1.6 and 1.7

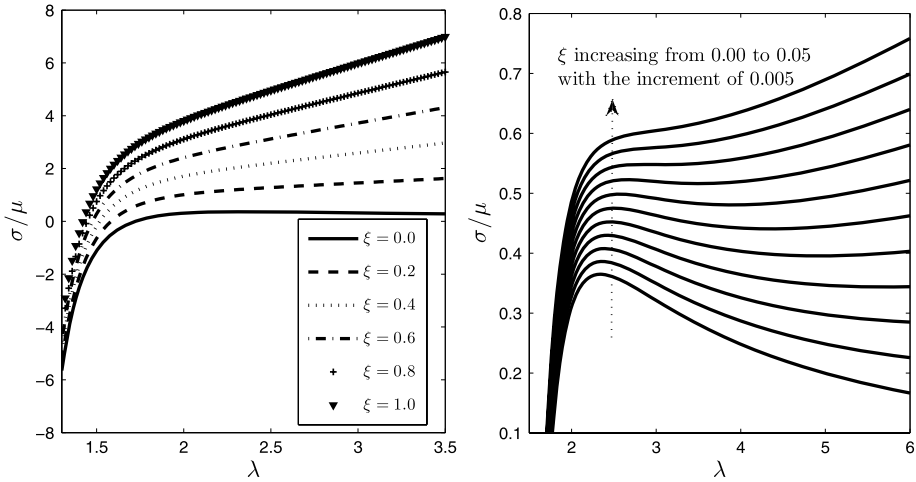

(a) σ/μ versus λ (b) Magnified portion of (a)

Fig. 9 Stress–stretch behavior for equitriaxial loading of a saturated gel with $\bar{M} = 100$ and $\chi = 0.425$ showing the effect of different ξ. For $\xi > 0.038$ the graphs are monotonic. For $0 < \xi < 0.038$ the graphs are decreasing on a finite interval in ξ

Thus (40) with $\sigma = 0$ and $J = 1/v_{fs}$ retrieves (12). As one would anticipate, $\sigma > 0$ implies $J > 1/v_{fs}$ and vice-versa. Consider again $\bar{M} = 100$ and $\chi = 0.425$. The graph of σ vs. $\lambda = J^{1/3}$ is then found to be monotonically increasing provided $\xi > 0.038$. However if $\xi < 0.038$ we find that the graph of σ vs. λ exhibits a stress maximum (Fig. 9). For $0 < \xi < 0.038$ the stress maximum is followed by stress minimum, after which the stress is once again monotonically increasing. For $\xi = 0$ the stress is monotonically decreasing to zero as $\lambda \to \infty$.

Similar behavior occurs for values of $\bar{M} = M/\mu$ and χ that are close to $(\bar{M}, \chi) = (100, 0.425)$. Specifically, it is found that the graph of σ vs. $\lambda = J^{1/3}$ is monotonically

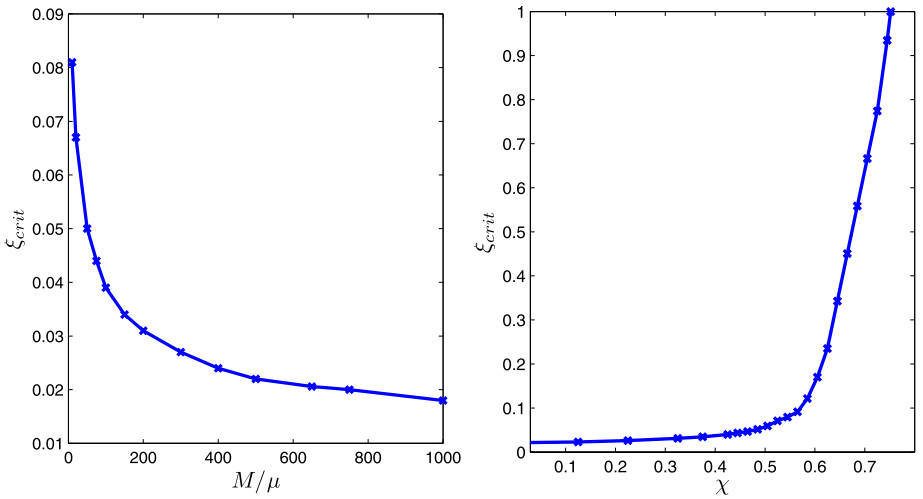

(a) ξ_{crit} versus $\bar{M}$ with $\chi = 0.425$ (b) ξ_{crit} versus χ with $\bar{M} = 100$

Fig. 10 Critical value ξ_{crit} for the existence of a local stress maximum in the equitriaxial stress response. For $\xi > \xi_{crit}$ the response is monotonic

increasing for all λ only if ξ is greater than a critical value ξ_{crit}. This critical value varies with both $\bar{M}$ and χ (see Fig. 10). For certain values of $\bar{M}$ and χ it is found that $\xi_{crit} = 1$ meaning that there always exists a local maximum in the stress response for equitriaxial loading. This occurs for example if $\bar{M} = 100$ and $\chi \geq 0.752$ as can be seen from Fig. 10b.

As is well known in hyperelasticity in general, nonmonotone stress response behavior of the type encountered here when $\bar{M} = 100$, $\chi = 0.425$, and $0 \leq \xi < 0.038$ is implicated in various loss of stability phenomena. Such issues are beyond the scope of this article. In contrast, for $\bar{M} = 100$, $\chi = 0.425$, and $\xi > 0.038$ no such issues arise. Then, J increases with σ and loss of saturation occurs at the constraining value $J = J_*$ when $\sigma = \sigma^*_{eqtri} \equiv \mu[(1-\xi)J_*^{-1/3} + 2\xi J_*^{1/3}] + M[J_*^{-1} + \chi J_*^{-2} + \ln(1 - J_*^{-1})]$. For $\sigma \geq \sigma^*_{eqtri}$ no additional expansion is possible, and the deformation gradient is therefore stalled at $\mathbf{F} = J_*^{1/3}\mathbf{I}$. The reactive pressure $-p$ in (24) then renders the equitriaxial stress σ as formally indeterminant for $J = J_*$ (see dashed curves in Fig. 11).

4.4 Some Energy Considerations

We close this section on homogeneous deformation with some remarks upon the energetic aspects of saturated response vs. nonsaturated response. A standard expectation would be that a saturated response would minimize an appropriate energy with respect to all nonsaturated responses, since the former is able to take on any value of J. We consider this issue in the context of uniaxial response, since that case offered the intriguing behavior such that, for certain ξ, there could be a load induced loss-of-saturation followed later by a load induced regain-of-saturation. Following the previous development in Sect. 4.2, we again restrict attention to deformations that preserve uniaxial symmetry and we also assume that there is sufficient liquid for a saturated free swelling.

Consider a unit cube that is oriented with respect to $(\mathbf{e}_1, \mathbf{e}_2, \mathbf{e}_3)$ prior to swelling and prior to the application of load. After free swelling, let the two sides with normal $\mathbf{e}_1$ be subject

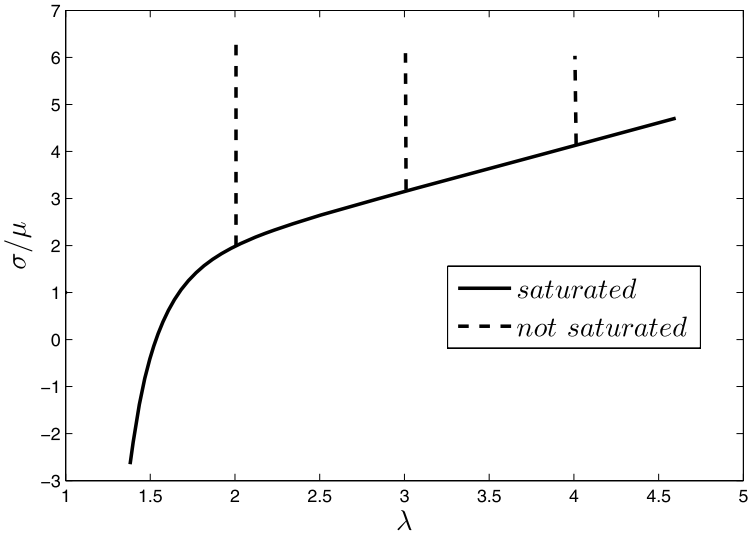

Fig. 11 Stress–stretch behavior for equitriaxial loading with $\bar{M} = 100$, $\chi = 0.425$, and $\xi = 0.5$ showing three examples of nonsaturated response. Since the stretch $\lambda = J^{1/3}$, no additional stretch is possible after loss of saturation

to a uniform normal traction with resultant normal force P and let the four remaining sides be traction free. The cube is deformed into a rectangular parallelepiped with stretch ratios $\lambda_1 = \lambda$ and $\lambda_2 = \lambda_3 = \sqrt{J/\lambda}$. One may distinguish between either a hard loading device or a soft loading device. In the hard device, λ is regarded as given. For the soft loading device, P is regarded as given.

The energy to be minimized for the hard device is simply the stored energy density as given by the integral of $W(\mathbf{F})$ over the reference configuration. Since the reference configuration is the unit cube, it follows from (10) that

$$E_{hard} = \bar{E}_{hard}(\lambda, J) \equiv \Phi(\lambda^2 + 2J/\lambda, 2\lambda J + J^2/\lambda^2, J) + H(J). \tag{41}$$

For Φ given by (11) the expression for $\bar{E}_{hard}$ is

$$\bar{E}_{hard}(\lambda, J) = \frac{\mu}{2}\left[(1-\xi)\left(\lambda^2 + \frac{2J}{\lambda} - 3\right) + \xi\left(2J\lambda + \frac{J^2}{\lambda^2} - 3\right)\right] + H(J). \tag{42}$$

For the hard device, one minimizes $\bar{E}_{hard}(\lambda, J)$ with respect to J at fixed λ. Formally, the first step in the minimization involves seeking solutions to

$$\frac{\partial}{\partial J}\bar{E}_{hard} = 0, \tag{43}$$

which gives an equation for J provided that J obeys $J \leq J_*$. Notice that (43) with (42) retrieves (33).

The soft device energy expression differs from the hard device expression by subtracting the work that is done on the gel by the loading device. This represents the change in potential energy of a conservative loading device so that the system under consideration involves both

gel and loading device. The work of the load P on the unit cube is $P(\lambda - 1)$ so that

$$E_{soft} = \bar{E}_{soft}(\lambda, J, P) \equiv \bar{E}_{hard}(\lambda, J) - P(\lambda - 1). \tag{44}$$

For the soft device, one minimizes $\bar{E}_{soft}(\lambda, J, P)$ with respect to both J and λ at fixed P. Formally, the first step in the minimization involves seeking solutions to

$$\frac{\partial}{\partial J}\bar{E}_{soft} = 0, \quad \text{and} \quad \frac{\partial}{\partial \lambda}\bar{E}_{soft} = 0. \tag{45}$$

Using $\bar{E}_{soft} = \bar{E}_{hard} - P(\lambda - 1)$ it follows that (45) is equivalent to

$$\frac{\partial}{\partial J}\bar{E}_{hard} = 0, \quad \text{and} \quad \frac{\partial}{\partial \lambda}\bar{E}_{hard} - P = 0. \tag{46}$$

Since $P = \sigma\lambda_2\lambda_3 = \sigma J/\lambda$ one verifies for Φ given by the Mooney-Rivlin form (11) that (46) is the same as (32) and (33).

Thus both the hard and soft device analysis retrieves the saturation relation (33) between λ and J for uniaxial stress. This is a standard type of argument in hyperelasticity, although in the present context of a saturated gel it permits the determination of the fluid fraction $(1 - 1/J)$. In addition, the soft device analysis gives the load that is necessary to support this deformation. These relations hold so long as $J \leq J_*$. If, however, the solution to the above equations require that $J > J_*$ then the minimization is found to be given by taking $J = J_*$. In this case the gel is not saturated. Viewed in this fashion, the nonsaturated minimization occurs on the boundary of the minimization domain. It follows that a nonsaturated solution can never provide a lower minimum than that of the saturated solution, since the saturated minimization is able to explore a larger space of J values. Such considerations arise generally if a hyperelastic material is composed of a mixture of substances where one or more of them (here the liquid) is in limited supply.[5]

For specified λ, let the solution to (43) be $J = \bar{J}_{sat}(\lambda)$. Figure 12a displays $\bar{E}_{hard}(\lambda, \bar{J}_{sat}(\lambda))$ vs. λ for the standard constitutive forms (4) and (11) with $\xi = 1$. This is the hard device energy associated with liquid saturation in uniaxial stress. This panel also displays the nonsaturated hard device energies $\bar{E}_{hard}(\lambda, J_*)$ that are associated with the transitions previously displayed in Fig. 8. The nonsaturated gels involve more energy than the saturated gel, although it is a small effect in the figures. The saturated hard device energy $\bar{E}_{hard}(\lambda, \bar{J}_{sat}(\lambda))$ takes on its smallest value at $\lambda = \zeta$ which corresponds to free swelling.

In this context it is instructive to consider the graph of uniaxial load P as a function of λ for both saturated and nonsaturated response, again using the constitutive forms (4) and (11). The relation between P and λ for saturated response follows from (32) and (33) using $P = \sigma J/\lambda$. The graph of this relation now supplies a backbone curve. The corresponding relation between P and λ for nonsaturated response follows from (34) using $P = \sigma J_*/\lambda$. Since the reference area of the unit cube is unity, it follows that the load P is simply the first Piola-Kirchhoff stress T, which we recall appeared previously in (37) and (38) for the case of the $\xi = 0$ gel. For general ξ it follows on the basis of the above considerations that

$$P_{non} - P_{sat} = \mu(J - J_*)\left[(1 - \xi)\frac{1}{\lambda^2} + \xi\left(\frac{J_* + J}{\lambda^3} - 1\right)\right]. \tag{47}$$

[5] See e.g., [2] for a such a consideration when the substances in the elastic mixture are capable of chemical reaction.

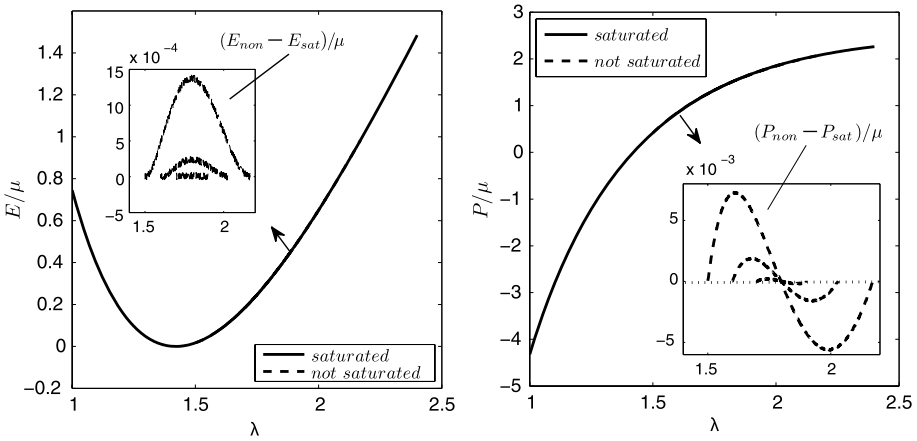

(a) E_{hard} versus λ (b) P versus λ

Fig. 12 Comparison of a saturated and a nonsaturated gel under uniaxial load. On the *left* is a comparison of the hard device energy expression. On the *right* is the resultant force as a function of stretch. As in Fig. 8 the constitutive parameters are given by $\bar{M} = 100$, $\chi = 0.425$ and $\xi = 1$. The transitions are taken to occur at $\lambda = 1.5$, 1.6 and 1.7

Here $J = J(\lambda)$ follows from (33), and so is given by the function $J = \bar{J}_{sat}(\lambda)$ as defined above.

Consider again the case that is associated with Fig. 12 in which the nonsaturated response is confined to the interval $\lambda^*_{uni-A} \le \lambda \le \lambda^*_{uni-B}$ where λ^*_{uni-A} and λ^*_{uni-B} depend upon J_*. The graph of the P vs. λ saturated backbone curve is depicted in Fig. 12b along with the nonsaturated P vs. λ curves on the finite intervals of nonsaturation. The nonsaturated curves depart and rejoin the backbone curve at λ^*_{uni-A} and λ^*_{uni-B}. It is noted however that there is an intermediate value of λ at which each nonsaturated curve crosses the backbone saturation curve. The nonsaturated response is first above the saturated response and then below the saturated response. It follows from (47) that the crossing value of λ is a root to $(1-\xi)/\lambda^2 + \xi((J_* + J)/\lambda^3 - 1) = 0$. This crossing value of λ depends on J_* and we find that it occurs before the value of λ that gives J_{max} for saturated response.

Here it is useful to note that the ordinary derivative of $\bar{E}_{hard}(\lambda, \bar{J}_{sat}(\lambda))$ with respect to λ gives, after use of the chain rule and application of both results from (46), that

$$P = \frac{d}{d\lambda}\bar{E}_{hard}(\lambda, \bar{J}_{sat}(\lambda)), \quad \text{(saturated)}. \tag{48}$$

The corresponding result for the nonsaturated force–stretch response at any fixed value J_* is given by

$$P = \frac{d}{d\lambda}\bar{E}_{hard}(\lambda, J_*), \quad \text{(not saturated)}. \tag{49}$$

Combining (48) and (49) gives a generalization of (47) in the form

$$P_{non} - P_{sat} = \frac{d}{d\lambda}\big(\bar{E}_{hard}(\lambda, J_*) - \bar{E}_{hard}(\lambda, \bar{J}_{sat}(\lambda))\big). \tag{50}$$

We may use (50) to show that the crossing exhibited in Fig. 12b is not tied to the particular constitutive forms (4) and (11). Consider any $H(J)$ and $\Phi(I_1, I_2, J)$ such that the saturated

uniaxial response gives a local maximum in the relation between J and λ. In such a case, if J_* as given in (9) is somewhat[6] less than the maximum value of J, then there will be an interval of nonsaturation which will again be denoted by $\lambda^*_{uni-A} \le \lambda \le \lambda^*_{uni-B}$. In particular, $\bar{J}_{sat}(\lambda^*_{uni-A}) = \bar{J}_{sat}(\lambda^*_{uni-B}) = J_*$. Integration of (50) now gives

$$\int_{\lambda^*_{uni-A}}^{\lambda^*_{uni-B}} (P_{non} - P_{sat})\, d\lambda = \left(\bar{E}_{hard}(\lambda, J_*) - \bar{E}_{hard}(\lambda, \bar{J}_{sat}(\lambda)) \right) \Big|_{\lambda^*_{uni-A}}^{\lambda^*_{uni-B}} = 0 - 0 = 0. \tag{51}$$

It thus follows that there is zero net area between the saturated force curve and each nonsaturated force curve on the finite interval of nonsaturation. Thus crossing of the saturated and nonsaturated force–stretch response curves must occur within the finite interval of nonsaturation.

5 The Inhomogeneous Deformation of an Everted Tube under Axial Load

For inhomogeneous deformation, the spatially varying stress field must satisfy the equations of equilibrium (15). For the constitutive forms (4) and (11) the Cauchy stress tensor is given by either (21) or (22) depending on whether the material is saturated or not saturated. The only difference between these two formulae is due to the presence of p in the nonsaturated Cauchy stress (22). Recalling that this p does not vary with location, it follows that $\operatorname{div}(-p\mathbf{I}) = -\nabla p = 0$. Thus the equilibrium equations $\operatorname{div} \boldsymbol{\sigma} = \mathbf{0}$ are the same whether the gel is saturated or not saturated. The distinction in mechanical response is due to the requirement (18) which causes the gel to obey the constraint $V = V_p + V_f$ (viz. (16), (17)) when it is no longer saturated. In the formal mathematical procedure, this constraint is met by the presence of p in the boundary conditions. These issues will be demonstrated for the inhomogeneous deformation of an everted tube subject to axial load. We shall continue to use the Flory-Huggins constitutive form (4) for H and the Mooney-Rivlin constitutive form (11) for Φ.

5.1 Formulation of the Everted Tube Problem

Consider a hollow circular cylinder using polar coordinates in the reference configuration $\Omega_{\mathbf{X}}$ with

$$R_i \le R \le R_o, \quad 0 \le \Theta < 2\pi, \quad 0 \le Z \le L, \quad (R_o > R_i > 0). \tag{52}$$

Let it then be immersed in the fluid. In the absence of external tractions the gel undergoes free swelling. Provided that sufficient liquid is available for saturation, the deformation of the freely swollen gel cylinder is described in polar coordinates $(\hat{r}, \hat{\theta}, \hat{z})$ as

$$\hat{r} = \zeta R, \quad \hat{\theta} = \Theta, \quad \hat{z} = \zeta Z. \tag{53}$$

Here ζ is again the free swelling stretch ratio as defined in (13).

Next, the swollen cylinder is everted (turned inside-out). The resulting deformation is described with respect to polar coordinates (r, θ, z) obeying $r_i \le r \le r_o$, $0 \le \theta < 2\pi$ by

$$r = f(\hat{r}), \quad \theta = \hat{\theta}, \quad z = -\hat{\lambda}_z \hat{z}, \quad (\hat{\lambda}_z > 0). \tag{54}$$

[6] To be more precise, there will be a neighborhood for J_* whose upper limit is the maximum value of J and whose lower limit is dependent on the details of the local maximum.

Combining (53) and (54) gives the transformation from the unswollen state (R, Θ, Z) to the swollen everted state (r, θ, z):

$$r = f(\zeta R) = r(R), \quad \theta = \hat{\theta} = \Theta, \quad z = -\lambda_z Z, \tag{55}$$

with

$$r_i \le r \le r_o, \quad 0 \le \theta < 2\pi, \quad -l \le z \le 0, \tag{56}$$

where $\lambda_z = \hat{\lambda}_z \zeta > 0$ and $l = \lambda_z L$. The presence of the minus sign in the expression for z in (54) gives rise to the eversion, and we seek solutions such that $f' < 0$ so that $r' < 0$. In particular, it follows that

$$r(R_i) = r_o, \quad r(R_o) = r_i. \tag{57}$$

For now, λ_z is regarded as a free parameter. It will ultimately be associated with the axial load on the ends $z = -l$ and $z = 0$.

The deformation gradient tensor associated with the mapping (55) is $\mathbf{F} = r'\mathbf{e}_r \otimes \mathbf{e}_R + (r/R)\mathbf{e}_\theta \otimes \mathbf{e}_\Theta - \lambda_z \mathbf{e}_z \otimes \mathbf{e}_Z$ where $\mathbf{e}_r, \mathbf{e}_\theta, \mathbf{e}_z$ and $\mathbf{e}_R, \mathbf{e}_\Theta, \mathbf{e}_Z$ are respectively the cylindrical polar unit basis vectors in the deformed and reference configurations, and $r' = dr/dR$. It then follows that

$$I_1 = r'^2 + \left(\frac{r}{R}\right)^2 + \lambda_z^2, \qquad I_2 = \left(\frac{r'r}{R}\right)^2 + \left(r'\lambda_z\right)^2 + \left(\frac{r}{R}\lambda_z\right)^2, \qquad J = -\frac{r'r}{R}\lambda_z. \tag{58}$$

For the constitutive relations (11) and (4) it follows from (21) that, for saturated response, there are no shear stresses and that the normal stresses are given by

$$\sigma_{rr} = -\mu\frac{Rr'}{\lambda_z r}\left[(1-\xi) + \xi\left(\frac{r}{R}\right)^2 + \xi\lambda_z^2\right] + M\left[\frac{-R}{\lambda_z r r'} + \chi\left(\frac{R}{\lambda_z r r'}\right)^2 + \ln\left(1 + \frac{R}{\lambda_z r r'}\right)\right], \tag{59}$$

$$\sigma_{\theta\theta} = -\mu\frac{r}{\lambda_z R r'}\left[(1-\xi) + \xi\lambda_z^2 + \xi r'^2\right] + M\left[\frac{-R}{\lambda_z r r'} + \chi\left(\frac{R}{\lambda_z r r'}\right)^2 + \ln\left(1 + \frac{R}{\lambda_z r r'}\right)\right], \tag{60}$$

$$\sigma_{zz} = -\mu\frac{R\lambda_z}{r r'}\left[(1-\xi) + \xi r'^2 + \xi\left(\frac{r}{R}\right)^2\right] + M\left[\frac{-R}{\lambda_z r r'} + \chi\left(\frac{R}{\lambda_z r r'}\right)^2 + \ln\left(1 + \frac{R}{\lambda_z r r'}\right)\right]. \tag{61}$$

For nonsaturated response a common constant p is to be subtracted from these normal stress expressions.

With the above stresses, the equilibrium equations associated with the θ and z directions are satisfied identically. The equilibrium equation associated with the r direction is

$$\frac{d}{dr}\left\{-\mu\frac{Rr'}{\lambda_z r}\left[(1-\xi) + \xi\left(\frac{r}{R}\right)^2 + \xi\lambda_z^2\right] + M\left[\frac{-R}{r r'\lambda_z} + \chi\left(\frac{R}{r r'\lambda_z}\right)^2 + \ln\left(1 + \frac{R}{r r'\lambda_z}\right)\right]\right\}$$
$$- \frac{\mu R}{\lambda_z r^2 r'}\left[(1-\xi) + \xi\lambda_z^2\right]\left[r'^2 - \left(\frac{r}{R}\right)^2\right] = 0. \tag{62}$$

The lateral surfaces of the everted tube are taken to be free of external tractions so that

$$\sigma_{rr}(r_i) = 0, \quad \sigma_{rr}(r_o) = 0. \tag{63}$$

Rearrangement of (62) yields a second order ODE for $r(R)$ in the form

$$r'' = -\frac{2\xi\frac{rr'^2}{R^2}(r'R - r) + \frac{r'}{r}[(1-\xi) + \xi\lambda_z^2][r'^2 - (\frac{r}{R})^2] + \lambda_z(\frac{r'^2}{R} - \frac{rr'}{R^2})F(R, r, r', \lambda_z)}{2r'[(1-\xi) + \xi(\frac{r^2}{R^2} + \lambda_z^2)] + \frac{\lambda_z r}{R}F(R, r, r', \lambda_z)} \tag{64}$$

where the function $F(R, r, r', \lambda_z)$ is defined by

$$F(R, r, r', \lambda_z) = \frac{r'^2[(1-\xi) + \xi(\frac{r^2}{R^2} + \lambda_z^2)]}{J} - \frac{M}{\mu}\left(\frac{1}{J(J-1)} - \frac{2\chi}{J^2}\right) \tag{65}$$

and J is given by $(58)_3$. Thus (64) with (63) provides an apparently well posed problem for $r(R)$. The solution describes an everted cylinder of saturated material so long as the condition (18) is met. The solution is dependent upon constitutive parameters: μ, M, χ, ξ, and upon the stretch parameter λ_z.

The solution to this problem will generally give a radially varying σ_{zz}. In particular, a condition of σ_{zz} being identically zero is not anticipated for any combination of parameters. This is connected to the observed behavior in eversion type deformations on rubbery materials mentioned in the Introduction. Namely, some flaring out of the top and bottom of an everted cylinder are observed in the absence of any tractions on the top and bottom surfaces. Thus the observed traction free deformations are not in accord with the simple eversion deformation (54). This suggests that tractions on the top and bottom surface caps would be necessary to sustain the simple eversion deformation. The deformation constructed on the basis of (64) with (63) is consistent with these expectations.

The normal stress σ_{zz} generates an overall axial force on the everted cylinder. Normalizing this axial force by the original surface area of the caps gives

$$P_{cap} \equiv \frac{2\pi}{\pi(R_o^2 - R_i^2)}\int_{r_i}^{r_o} r\sigma_{zz}dr. \tag{66}$$

It is to be noted that r_i and r_o defined in (57) are unknown before the solution is obtained. For fixed material parameters, P_{cap} will depend upon λ_z. The force-stretch relation P_{cap} vs. λ_z is analogous to the homogeneous deformation relation in uniaxial stress between P and λ discussed in the previous section. Recall that this is given in general by (48), where the specialization to the Mooney-Rivlin constitutive form uses (42). In particular, one may then compare the relation between P and λ obtained from (48), to the relation between P_{cap} and λ_z obtained on the basis of (66) after the solution of (63) and (64). The former gives the force–stretch relation for the cylinder before it is everted so long as it remains saturated. The latter gives the force–stretch relation for the cylinder after it is everted so long as it too remains saturated.

5.2 Numerical Results for a Saturated System

We have integrated the differential equation (64) after suitable nondimensionalization by means of a fourth order Runge-Kutta method using the same material parameters: $\chi = 0.425$, $\bar{M} = M/\mu = 100$ that were employed in the homogeneous deformation study.

A shooting procedure was used to meet the two point boundary conditions. The unswollen configuration was taken to involve $R_o/R_i = 2$. Calculations were performed for different values of ξ and hence different values of the free swelling stretch ζ. For each such ξ, the problem was solved numerically for a sequence of $\hat{\lambda}_z$, which it is recalled is the mechanical portion of the mechanical stretch ratio that appears in (54).

Radial deformation of the everted cylinder is shown in Fig. 13(a) and (c) for the respective cases $\xi = 0$ and $\xi = 1$. Here the horizontal axis represents dimensionless radial coordinates $\bar{R} \equiv R/R_i$ in the reference configuration while the vertical axis gives the dimensionless radial coordinates $\bar{r} \equiv r/(\zeta R_i)$ in the deformed configuration. As $\hat{\lambda}_z$ increases, it is found that both the deformed inner and outer radii decrease, which is consistent with the expectation of a transverse contraction under axial extension. Figure 13(b) and (d) shows the radial variation of J (normalized by ζ^3) which gives the gel's local volume change and hence the amount of fluid absorbed into the cylinder. It is to be noticed in panels (b) and (d) that the horizontal axis represents the deformed radial coordinate $\bar{r}$ and so the curves start and end at different locations on the horizontal axis. For each value of mechanical stretch $\hat{\lambda}_z$, the volume change is relatively greater near the outer periphery, indicating that the volume fraction of liquid increases with radius in the everted cylinder.

Graphs of the normal stresses are displayed in Fig. 14 for both $\xi = 0$ and $\xi = 1$ at a variety of mechanical stretches $\hat{\lambda}_z$. Note that $\sigma_{rr} < 0$ in the interior of the everted cylinder. The hoop stress $\sigma_{\theta\theta}$ is found to be compressive in the inner portion of the cylinder and tensile in the outer portion (which is broadly consistent with the notion that the liquid is "squeezed" toward the outer portion). The axial stress σ_{zz} also exhibits radial variation and correlates with stretch $\hat{\lambda}_z$ in the anticipated fashion. The qualitative form for all of the curves is shown to be quite sensitive to the value of ξ.

The relation between $\hat{\lambda}_z$ and P_{cap} as defined in (66) is shown by the solid curves in Fig. 15(a) and Fig. 15(c) for $\xi = 0$ and $\xi = 1$, respectively. These are compared with the uniaxial loading (without eversion) as represented by the dashed curves in the same panels. For the neo-Hookean type gel ($\xi = 0$), the everted cylinder undergoes greater elongation at a given load than does the uneverted cylinder. However, the opposite occurs for $\xi = 1$. Panels (b) and (d) of Fig. 15 show how the total cylinder volume varies with mechanical stretch, again for the respective cases $\xi = 0$ and $\xi = 1$. Specifically, the total volume as given by (17) is normalized by the free swelling volume (solid curve), and compared to the normalized volume of the uneverted cylinder (dashed curve). The total volume of the uneverted cylinder is determined by the value of J in the homogeneous deformation for uniaxial stress. This value of J was previously displayed (vs. overall stretch) in Fig. 6(b) using the now standard constitutive parameters $\bar{M} = 100$ and $\chi = 0.425$. Recall for uniaxial stress that the relation between J and stretch was not monotonic for $\xi > 0$. Thus the dashed curve in Fig. 15(d) is not monotonic. It is to be observed from panel (b) of Fig. 15 that the everted cylinder for $\xi = 0$ preserves the monotonic relation between volume and stretch that was found in the uneverted cylinder. Similarly, panel (d) of Fig. 15 shows that the everted cylinder for $\xi = 1$ gives a relation between volume and stretch that is not monotonic as was the case for the uneverted cylinder with $\xi = 1$. It is also interesting to note for both $\xi = 0$ and $\xi = 1$ that the total volume of the everted cylinder is less than that of an uneverted cylinder at the same value of stretch. Thus for both $\xi = 0$ and $\xi = 1$ the everted cylinder holds less fluid than the corresponding uneverted cylinder.

The form of the volume vs. stretch curves in panels (b) and (d) of Fig. 15 have immediate consequences as regards the possibility of loss of saturation. The results mirror the corresponding results for the uneverted cylinder, since the everted and uneverted curves in each

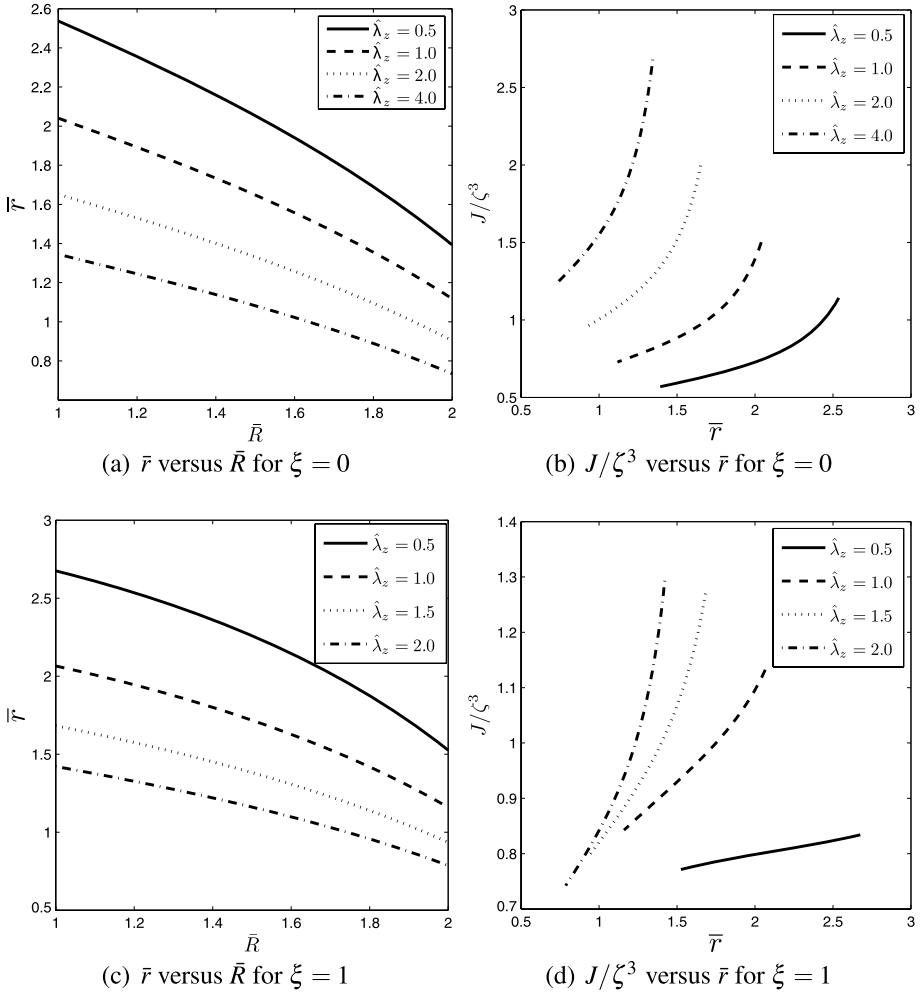

(a) $\bar{r}$ versus $\bar{R}$ for $\xi = 0$ (b) J/ζ^3 versus $\bar{r}$ for $\xi = 0$

(c) $\bar{r}$ versus $\bar{R}$ for $\xi = 1$ (d) J/ζ^3 versus $\bar{r}$ for $\xi = 1$

Fig. 13 Radial deformation ($\bar{r} = r/(\zeta R_i)$) and local volume change ratio as a function of radial position. As in previous figures, $\bar{M} = 100$ and $\chi = 0.425$. The cylinder geometry is such that $R_o = 2R_i$

panel display the same qualitative form. In general, the saturated solution holds provided that

$$\pi \lambda_z L(r_o^2 - r_i^2) \leq \pi L(R_o^2 - R_i^2) + V_f, \tag{67}$$

where it is recalled that $\lambda_z = \hat{\lambda}_z \zeta$. We now consider differences that occur for the respective cases $\xi = 0$ and $\xi = 1$ which stem from the different qualitative forms of the curves in panels (b) and (d) of Fig. 15.

Consider first the material with $\xi = 0$. The monotone curve for the everted cylinder in Fig. 15b then indicates that an everted cylinder of the $\xi = 0$ material will be saturated if $\hat{\lambda}_z$ is less than a critical value. Conversely, the everted cylinder will not be saturated if $\hat{\lambda}_z$ exceeds the critical value. The critical value of mechanical stretch is dependent upon the amount of available fluid, and can be directly determined with the aid of Fig. 15b. It is to be noted from

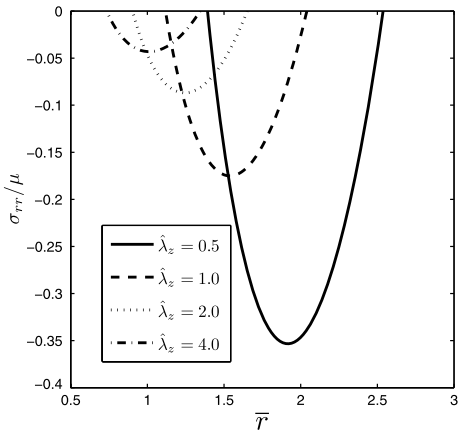

(a) σ_{rr} versus $\bar{r}$ for $\xi = 0$

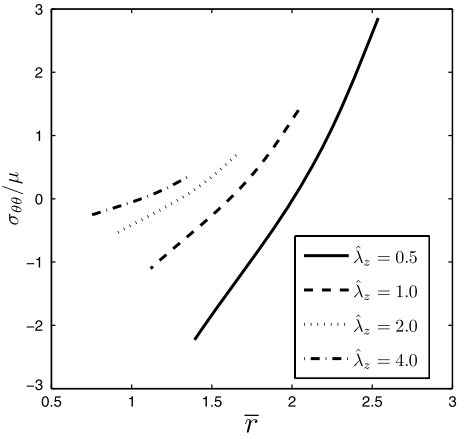

(b) $\sigma_{\theta\theta}$ versus $\bar{r}$ for $\xi = 0$

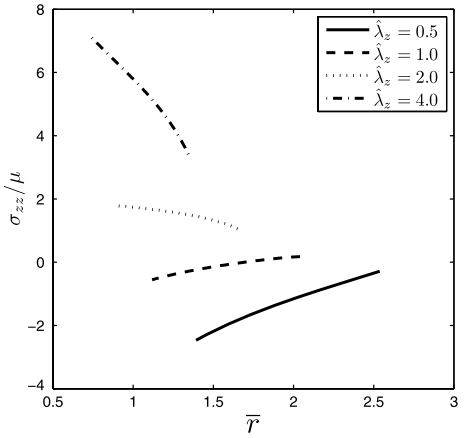

(c) σ_{zz} versus $\bar{r}$ for $\xi = 0$

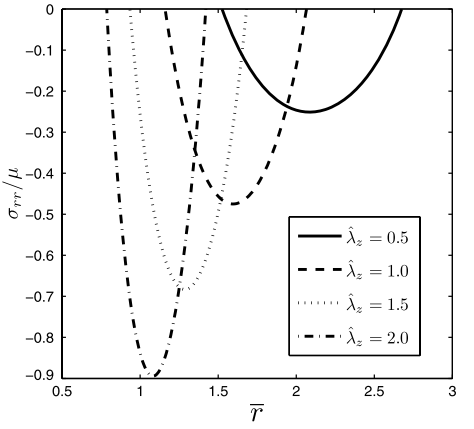

(d) σ_{rr} versus $\bar{r}$ for $\xi = 1$

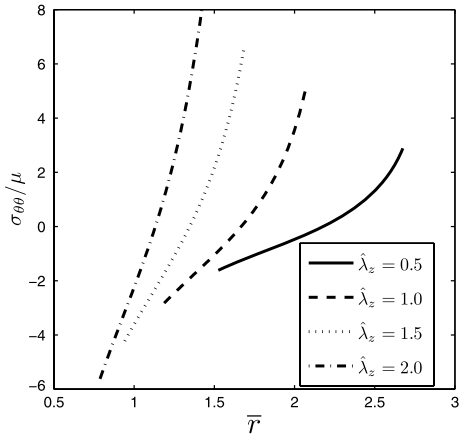

(e) $\sigma_{\theta\theta}$ versus $\bar{r}$ for $\xi = 1$

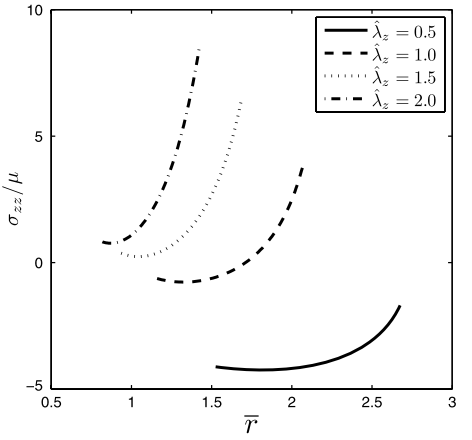

(f) σ_{zz} versus $\bar{r}$ for $\xi = 1$

Fig. 14 Radial distribution of normal stresses for the everted cylinder with $R_o = 2R_i$ using the same material parameters as in Fig. 13

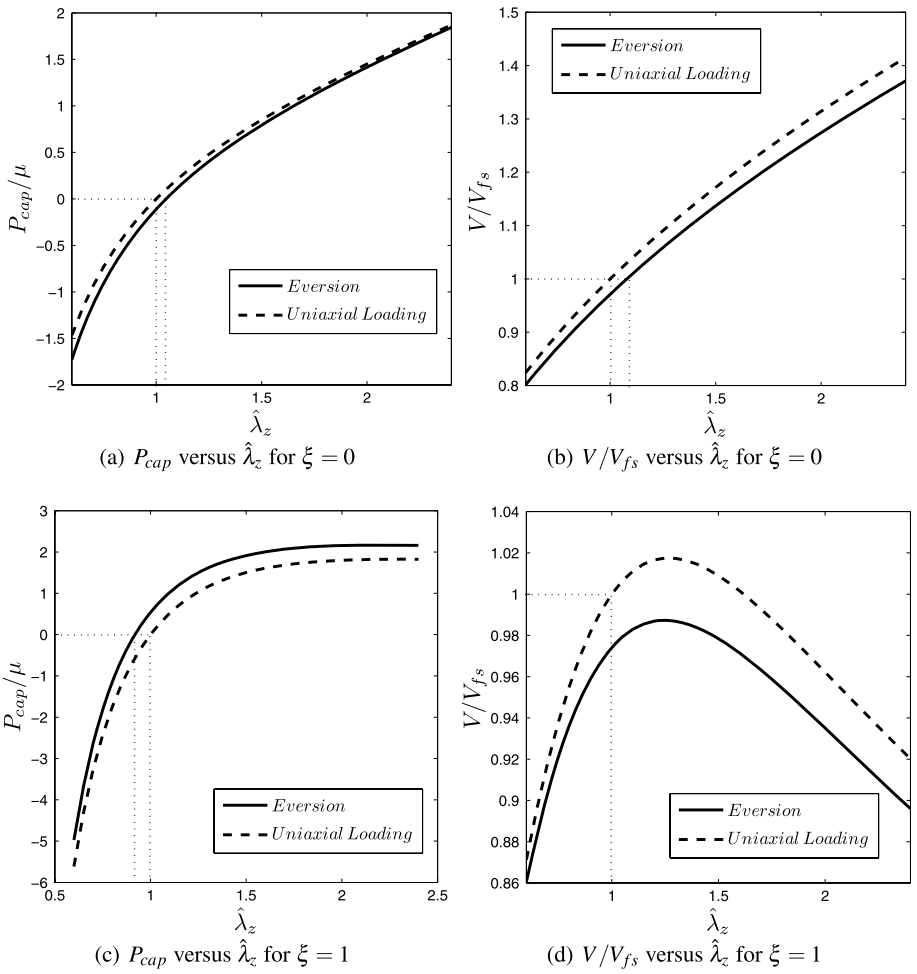

Fig. 15 Resultant axial force as a function of mechanical stretch and total volume as a function of mechanical stretch for both the everted cylinder and the uneverted cylinder using the same material parameters as in Fig. 13. For the everted cylinder, the reference geometry is again such that $R_o = 2R_i$

this figure that, for a given amount of fluid, the transition value of mechanical stretch for the everted cylinder exceeds the transition mechanical stretch value for the uneverted cylinder.

Consider now the material with $\xi = 1$. Then the graphs of volume vs. stretch for both the everted cylinder and the uneverted cylinder each have a local maximum. Consequences for the uneverted cylinder were discussed in Sect. 4.2[7] and similar considerations apply to the everted cylinder. Thus the everted cylinder will be saturated for all values of stretch if the amount of available fluid exceeds that associated with the value of the local maximum. If less than this amount of fluid is available, then there will be an interval of stretch for which the everted cylinder is not saturated. It is to be noted from Fig. 15d that the value of the local maximum for the uneverted cylinder gives $V > V_{fs}$ where V_{fs} is the free swelling

[7]See the paragraph between (38) and (39).

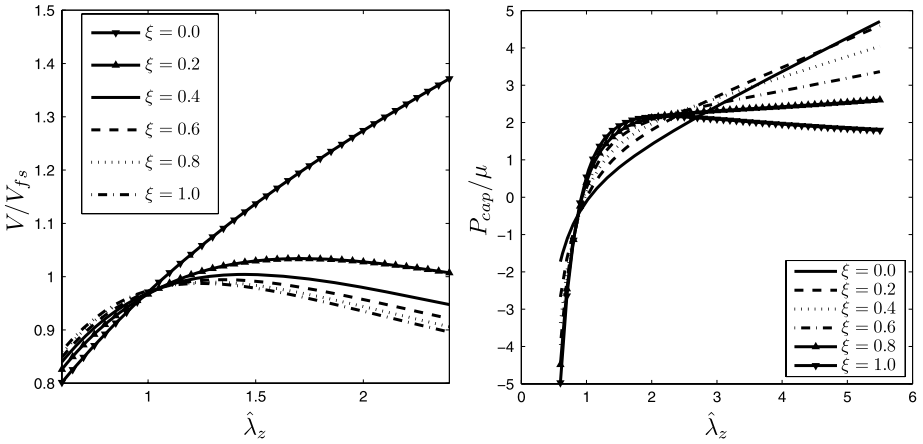

(a) V/V_{fs} versus $\hat{\lambda}_z$ (b) P_{cap} versus $\hat{\lambda}_z$

Fig. 16 Total volume after eversion as a function of mechanical stretch, and resultant force as a function of mechanical stretch, for various values of ξ, again using $\bar{M} = 100$, $\chi = 0.425$ and $R_o = 2R_i$

volume of the cylinder before eversion. Conversely, the value of the local maximum for the everted cylinder gives $V < V_{fs}$. Consider therefore two identical cylinders, each of which is removed from its liquid bath after free swelling so that the amount of fluid is fixed at the free swelling value. Let one of the two cylinders now suffer an eversion. This everted cylinder will remain saturated for any value of axial stretch. In comparison, the uneverted cylinder will immediately lose saturation if it is stretched a small amount. However, if the stretch of the uneverted cylinder becomes sufficiently large, then it too will regain saturation.

The above interpretation for a $\xi = 1$ gel is a consequence of the inequality $V < V_{fs}$ holding for all values of stretch in the everted cylinder. More generally, for $\xi > 0$ we find that the graph of stretch vs. overall volume continues to exhibit a local maximum. However, as shown in Fig. 16a, the value of V at the local maximum is found to be greater than the free swelling volume provided that this positive ξ is sufficiently small. For these materials it follows that a quantity of liquid just sufficient for free swelling gives rise to an everted cylinder that loses saturation on a finite interval of stretch. The relation between force and mechanical stretch for a saturated everted cylinder using the same values of ξ as in panel (a) of Fig. 16 is shown in panel (b) of this same figure. These serve as backbone curves for any nonsaturated response. In order to display force vs. stretch curves associated with loss of saturation it is necessary to solve the boundary value problem for an everted cylinder that is not saturated. We consider this issue in the next section.

6 The Everted Cylinder that is not Saturated

We now consider the consequences of a limited fluid supply for the eversion deformation. Specifically, if the total volume of a saturated, everted cylinder is calculated to be greater than $V_p + V_f$ then there is insufficient fluid for the cylinder to be saturated. The resulting nonsaturated solution obeys

$$\lambda_z(r_o^2 - r_i^2) = (R_o^2 - R_i^2) + \frac{V_f}{\pi L}, \tag{68}$$

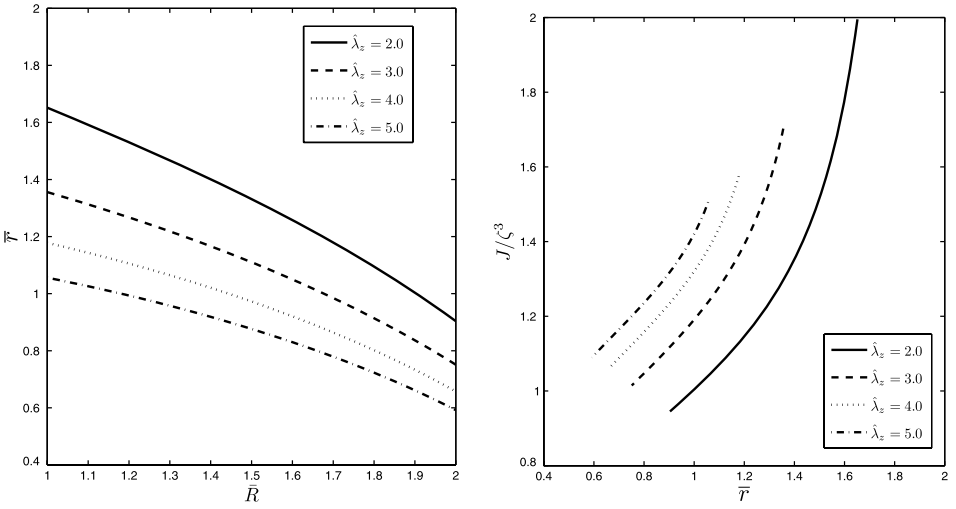

(a) $\bar{r}$ versus $\bar{R}$

(b) J/ξ^3 versus $\bar{r}$

(c) σ_{rr} versus $\bar{r}$

(d) $\sigma_{\theta\theta}$ versus $\bar{r}$

Fig. 17 Deformation and stress fields associated with loss of saturation for an everted cylinder with $R_o = 2R_i$. The material parameters are $\bar{M} = 100$, $\chi = 0.425$, and $\xi = 0$. Loss of saturation is taken to occur at $\hat{\lambda}_z^* = 2.0$. Thus the curves for $\hat{\lambda}_z = 2.0$ are the same as the corresponding curves for $\xi = 0$ that were displayed in Figs. 13 and 14. For $\hat{\lambda}_z > 2.0$ the curves in this figure differ from corresponding curves for a saturated gel

where it is recalled $\lambda_z = \hat{\lambda}_z \zeta$. As discussed previously, the stress equations of equilibrium are unchanged from that for a saturated system. Thus the displacement field $r(R)$ is still subject to (64) where F is given by (65). The normal stresses are modified by subtracting the common constant p from the saturated stress relations as previously given in (59)–(61). Eliminating this constant between the two conditions in (63) now gives

$$-\frac{R_i r_i'}{\lambda_z r_i}\left[(1-\xi)+\xi\left(\frac{r_i}{R_i}\right)^2+\xi\lambda_z^2\right]+\bar{M}\left[\frac{-R_i}{\lambda_z r_i r_i'}+\chi\left(\frac{R_i}{\lambda_z r_i r_i'}\right)^2+\ln\left(1+\frac{R_i}{\lambda_z r_i r_i'}\right)\right]$$

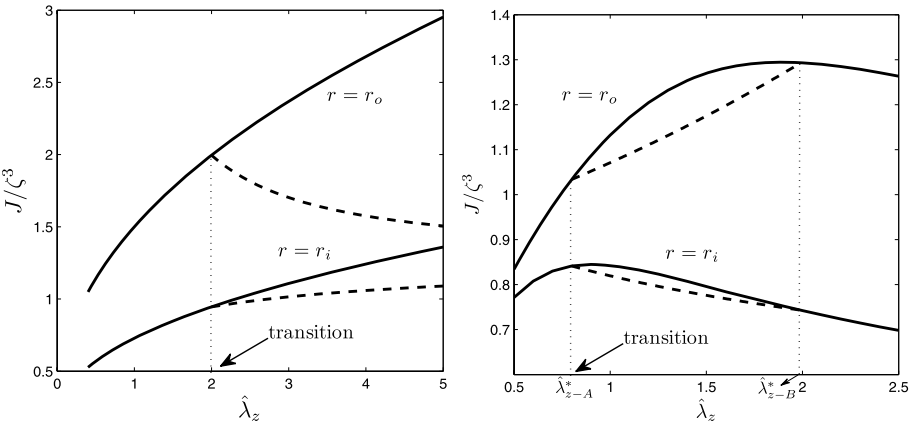

(a) $\xi = 0$ (b) $\xi = 1$

Fig. 18 Local volume change J versus $\hat{\lambda}_z$ for an everted cylinder with $R_o = 2R_i$ and material parameters $\bar{M} = 100$, $\chi = 0.425$ and either $\xi = 0$ or $\xi = 1$. On the *left*, $\xi = 0$ and the loss of saturation corresponds to that depicted in Fig. 17. After loss of saturation, increasing stretch redistributes the finite amount of fluid from the outer region to the inner region. On the *right*, $\xi = 1$ and the loss of saturation corresponds to that depicted in Fig. 19. For the nonsaturated cylinder, increasing stretch now redistributes the finite amount of fluid from the inner region to the outer region

$$= -\frac{R_o r_o'}{\lambda_z r_o}\left[(1-\xi) + \xi\left(\frac{r_o}{R_o}\right)^2 + \xi\lambda_z^2\right]$$
$$+ \bar{M}\left[\frac{-R_o}{\lambda_z r_o r_o'} + \chi\left(\frac{R_o}{\lambda_z r_o r_o'}\right)^2 + \ln\left(1 + \frac{R_o}{\lambda_z r_o r_o'}\right)\right], \tag{69}$$

where $r_i' = r'(R_i)$ and $r_o' = r'(R_o)$. The second order ODE (64) is to be solved subject to (68) and (69), after which p is obtained from (63).

For values V_f that cause the saturated solution condition (67) to be violated, we have solved (64) using a double shooting method so as to meet both (68) and (69). The solutions are dependent upon the mechanical stretch $\hat{\lambda}_z$ and the value of $V_f/\pi L$ appearing in (68). Each such $V_f/\pi L$ determines the range of $\hat{\lambda}_z$ for which there is loss of saturation. As discussed in the previous section, the range of nonsaturated $\hat{\lambda}_z$ can be unbounded (as in the $\xi = 0$ example of Fig. 15) or can be confined to a finite interval (as in the $\xi = 1$ example of Fig. 15).

Consider the material parameters associated with the $\xi = 0$ saturated solution fields that were previously displayed in Fig. 13 and Fig. 14. The relation between total volume and mechanical stretch for this material was displayed in panel (b) of Fig. 15. Since this relation is monotonically increasing, it follows that loss of saturation could occur for any value of stretch. Following previous convention, this transition value of stretch will be denoted $\hat{\lambda}_z^*$ and the nonsaturated solution therefore applies for $\hat{\lambda}_z \geq \hat{\lambda}_z^*$. Figure 17 displays the nonsaturated solution fields associated with this same material for the particular value of V_f that gives $\hat{\lambda}_z^* = 2.0$. Thus for this V_f the curves in Fig. 13 and Fig. 14 corresponding to $\hat{\lambda}_z \leq \hat{\lambda}_z^* = 2.0$ would continue to apply. However there would now be insufficient fluid to saturate the everted cylinder when $\hat{\lambda}_z > 2.0$ and so the $\hat{\lambda}_z = 4.0$ curves in Fig. 13 and Fig. 14 would no longer apply. Instead, the solution fields for $\hat{\lambda}_z = 4.0$ are as depicted in Fig. 17. The solution fields for the nonsaturated everted cylinder for other values of mechanical stretch

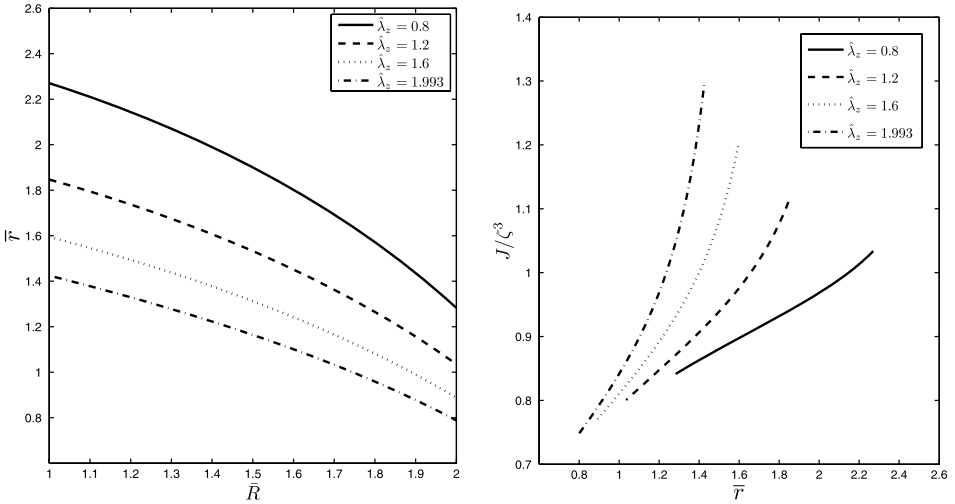

(a) $\bar{r}$ versus $\bar{R}$ (b) J/ξ^3 versus $\bar{r}$

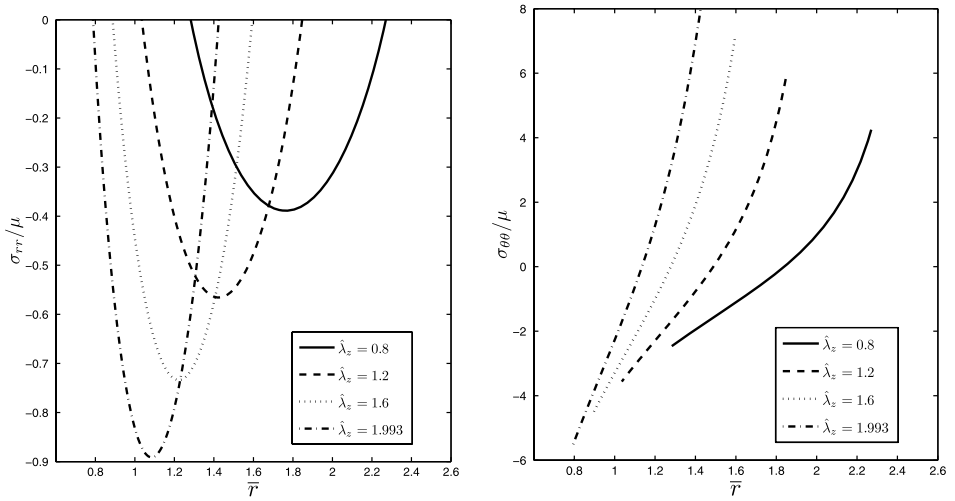

(c) σ_{rr} versus $\bar{r}$ (d) $\sigma_{\theta\theta}$ versus $\bar{r}$

Fig. 19 Deformation and stress fields associated with loss of saturation for an everted cylinder with $R_o = 2R_i$. The material parameters are $\bar{M} = 100$, $\chi = 0.425$, and $\xi = 1$. The value of V_f is such that loss of saturation occurs on the interval $0.8 \leq \hat{\lambda}_z \leq 1.993$

$\hat{\lambda}_z > \hat{\lambda}_z^*$ are also shown in Fig. 17. The nonsaturated solution is identical to the saturated solution at the transition stretch $\hat{\lambda}_z^*$ as is verified by comparison of the curves for $\hat{\lambda}_z = 2.0$ in Figs. 13, 14 and 17. As the mechanical stretch increases, comparison of Fig. 14 and Fig. 17 reveals similar qualitative trends in the nature of the stress fields after loss of saturation. In contrast, comparison of Fig. 13 and Fig. 17 shows qualitative differences in the J field after loss of saturation. Specifically, the saturated solution gives values of J that increase at each point in the everted cylinder. Hence all locations absorb additional fluid as $\hat{\lambda}_z$ increases so long as the gel is saturated. However, upon loss of saturation, it is found that the value of J now decreases on the outer portion of the cylinder (while continuing to increase in the inner

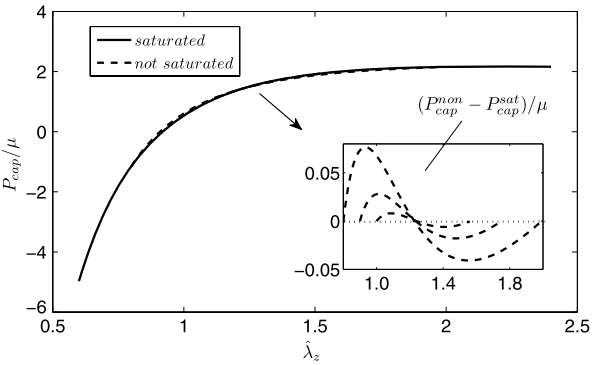

Fig. 20 Resultant axial force as a function of mechanical stretch for the everted cylinder with $R_o = 2R_i$. Material parameters correspond to those in Fig. 15(c), namely: $\bar{M} = 100$, $\chi = 0.425$, and $\xi = 1$. Three different values of V_f are considered, corresponding to $\hat{\lambda}_z^* = 0.8, 0.9$, and 1.0. The nonsaturated response curve is first above, and then below, the saturated response curve, and so mirrors the case of this material under homogeneous deformation (Fig. 12b)

portion of the cylinder). This is shown in detail in the first panel of Fig. 18. Thus, after loss of saturation, the fixed amount of fluid within the cylinder exhibits a quasi-static migration from the outer portion of the everted cylinder to the inner portion of the everted cylinder under increasing mechanical stretch $\hat{\lambda}_z$.

In a similar fashion Fig. 19 exhibits nonsaturated solution fields for the $\xi = 1$ material whose saturated solution fields were previously exhibited in Fig. 13 and Fig. 14. The relation between overall volume and mechanical stretch for this material is displayed in panel (d) of Fig. 15. Since this relation exhibits a local maximum it follows that loss of saturation occurs on a finite interval of stretch. Again, following previous convention, we denote the endpoints of this interval by $\hat{\lambda}_{z-A}^*$ and $\hat{\lambda}_{z-B}^*$. For the purposes of Fig. 19, we take $\hat{\lambda}_{z-A}^* = 0.8$ which in turn makes $\hat{\lambda}_{z-B}^* = 1.993$. Once again, the fixed amount of fluid redistributes itself in a quasi-static fashion as $\hat{\lambda}_z$ varies in the interval $\hat{\lambda}_{z-A}^* \leq \hat{\lambda}_z \leq \hat{\lambda}_{z-B}^*$. In particular, as $\hat{\lambda}_z$ increases through this interval we find that fluid migrates from the inner portion of the everted cylinder to the outer portion. This is shown in detail in the second panel of Fig. 18. For this material, after a return to saturation at $\hat{\lambda}_{z-B}^*$, any further increase in mechanical stretch gives a loss in overall volume, indicating that increasing mechanical stretch now expels fluid from the everted cylinder.

Recall for the fluid saturated everted cylinder that the relation between axial force and axial stretch was given previously in Fig. 15 for both the $\xi = 0$ material (panel a) and the $\xi = 1$ material (panel c). Loss of saturation causes the response to depart away from this backbone response. The question therefore arises as to whether this departure takes place in a manner that is similar to that which occurs in the homogeneous deformation of uniaxial stress. Recall for the homogeneous deformation of uniaxial stress that the departure of the nonsaturated axial force response from the saturated backbone response was displayed in Fig. 12b for the $\xi = 1$ material. The conspicuous feature of Fig. 12b was that the nonsaturated axial load response for the $\xi = 1$ material was first above, and then below, the saturated axial load response. We find that similar qualitative behavior occurs for the $\xi = 1$ material as the everted cylinder is mechanically stretched. This is shown in Fig. 20 where the difference between saturated and nonsaturated response is shown not only for the case in which $\hat{\lambda}_{z-A}^* = 0.8$, but also for two other cases corresponding to $\hat{\lambda}_{z-A}^* = 0.9$ and $\hat{\lambda}_{z-A}^* = 1.0$.

Acknowledgements We thank N.T. Wright, R. Monroe, a reviewer, and R. Fosdick for helpful discussions and comments. We acknowledge the support of the US National Science Foundation under Grant No. 0510600 to Michigan State University.

References

1. Baek, S., Srinivasa, A.R.: Diffusion of a fluid through an elastic solid undergoing large deformation. Int. J. Non-Linear Mech. **39**, 201–218 (2004)
2. Buonsanti, M., Fosdick, R., Royer-Carfagni, G.: Chemomechanical equilibrium of bars. J. Elast. **84**, 167–188 (2006)
3. Chen, Y.C., Haughton, D.M.: Existence of exact solutions for the eversion of elastic cylinders. J. Elast. **49**, 79–88 (1997)
4. Doi, M.: Introduction to Polymer Physics. Oxford Science Publications/Clarendon, Oxford (1996)
5. Flory, P.J.: Thermodynamics of high polymer solutions. J. Chem. Phys. **10**, 51–61 (1942)
6. Flory, P.J.: Statistical mechanics of swelling of network structures. J. Chem. Phys. **18**, 108–111 (1950)
7. Flory, P.J., Rehner, J.: The effect of deformation on the swelling capacity of rubber. J. Chem. Phys. **12**, 412–414 (1944)
8. Gandhi, M.V., Rajagopal, K.R., Wineman, A.S.: Some nonlinear diffusion problems within the context of the theory of interacting continua. Int. J. Eng. Sci. **25**(11–12), 1441–1457 (1987)
9. Gandhi, M.V., Usman, M., Wineman, A.S., Rajagopal, K.R.: Combined extension and torsion of a swollen cylinder within the context of mixture theory. Acta Mech. **79**, 81–95 (1989)
10. Haughton, D.M., Orr, A.: Further results for the eversion of highly compressible elastic cylinders. Math. Mech. Solids **1**, 355–367 (1996)
11. Haughton, D.M., Orr, A.: On the eversion of compressible elastic cylinders. Int. J. Solids Struct. **34**, 1893–1914 (1997)
12. Huggins, M.L.: Theory of solutions of high polymers. J. Am. Chem. Soc. **64**, 1712–1719 (1942)
13. Paul, D.R., Ebra-Lima, O.M.: Pressure-induced diffusion of organic liquids through highly swollen polymer membranes. J. Appl. Polym. Sci. **14**, 2201–2224 (1970)
14. Rajagopal, K.R., Srinivasa, A.R.: On the thermomechanics of materials that have multiple natural configurations part I: viscoelasticity and classical plasticity. Z. Angew. Math. Phys. **55**, 861–893 (2004)
15. Rajagopal, K.R., Tao, L.: Mechanics of Mixtures. World Scientific, Singapore (1995)
16. Rajagopal, K.R., Wineman, A.S., Gandhi, M.: On boundary conditions for a certain class of problems in mixture theory. Int. J. Eng. Sci. **24**(8), 1453–1463 (1986)
17. Rivlin, R.S.: Large elastic deformation of isotropic materials, vi. further results in the theory of torsion, shear and flexure. Phil. Trans. R. Soc. A **242**(845), 173–195 (1949)
18. Treloar, L.R.G.: The equilibrium swelling of cross-linked amorphous polymers. Proc. R. Soc. Lond. **A200**, 176–183 (1950)
19. Treloar, L.R.G.: Swelling of a rubber cylinder in torsion: part 1 theory. Polymer **13**, 195–202 (1972)
20. Treloar, L.R.G.: The Physics of Rubber Elasticity. Oxford University Press, Oxford (1975)
21. Treloar, L.R.G.: Swelling of bonded-rubber cylinders. Polymer **17**, 142–146 (1976)
22. Varga, O.H.: Stress-Strain Behavior of Elastic Materials. Interscience, New York (1966)
23. Wineman, A.S., Rajagopal, K.R.: Shear induced redistribution of fluid within a uniformly swollen nonlinear elastic cylinder. Int. J. Eng. Sci. **30**(11), 1583–1595 (1992)